Elucidation of B-N and B-P Stretching Vibrations Using Raman Spectroscopy and Electronic Structure Calculations

By:

Dana Nicole Reinemann

A thesis submitted to the faculty of the University of Mississippi in partial fulfillment of the requirements of the Sally McDonnell Barksdale Honors College.

Oxford
April 2012

Approved by:

_____
Advisor: Professor Nathan Hammer

_____
Reader: Professor Gregory Tschumper

_____
Reader: Professor Susan Pedigo

©2012
Dana Nicole Reinemann
ALL RIGHTS RESERVED

ACKNOWLEDGEMENTS

Many people in the Department of Chemistry and Biochemistry and the Department of Chemical Engineering here at the University of Mississippi were of great assistance during the work presented in this manuscript. I would like to thank the professors of chemical engineering for supporting me throughout my research endeavors in the chemistry department. Specifically, I would like to thank Dr. John O'Haver for his advisement throughout my college career. In the chemistry department, I would like to thank the research group of Dr. Gregory Tschumper for computational assistance and the Mississippi Center for Supercomputing Research for the use of their computational facilities. I would also like to thank graduate students Debra Jo Scardino and Ashley Wright for their support and advisement throughout this research project. Lastly, I would like to thank my advisor, Dr. Nathan Hammer, for allowing me to work in his laboratory as well as perform worthwhile research while fulfilling this thesis requirement.

ABSTRACT

DANA NICOLE REINEMANN: Elucidation of B-N and B-P Stretching Vibrations Using Raman Spectroscopy and Electronic Structure Calculations
(Under the direction of Dr. Nathan Hammer)

Boron-nitrogen (B-N) and boron-phosphorus (B-P) dative bond stretching vibrational frequencies were studied using vibrational spectroscopic methods and electronic structure calculations. There has been a great controversy over the assignment of B-N dative bond vibrational frequencies for many years with a range of inconsistent assignments in the literature. The B-N dative bond stretching frequency in *N*-methyliminodiacetic acid (MIDA) esters was analyzed here using infrared, Raman, and surface enhanced Raman spectroscopic methods and compared to the results of electronic structure calculations employing the MP2 and M06-2X methods with a triple zeta basis set. The mode including the B-N stretching motion proved to be fairly localized, even with the complex structure of this large molecule. Assignment was aided by performing a total energy distribution with the INTDER2005 program. The same approach was used to analyze B-P dative bond stretching vibrational frequencies in three molecules with large substitutions on the phosphorus atom. Although the B-P dative bond has been previously studied in many molecules, a trend connecting the structure of the molecules and the B-P stretching frequencies had not been determined. Employing Raman spectroscopy and electronic structure calculations, specifically with the M06-2X method, a systematic study of B-P molecules with various types of substitution is presented.

Table of Contents

1 Introduction 1

1.1 Dative Bonding and Applications 1

1.2 Spectroscopic Methods 3

1.2.1 Vibrational Spectroscopy 3

1.2.2 The Harmonic Oscillator 5

1.2.3 Normal Modes 7

1.2.4 Raman Spectroscopy 7

1.2.5 Surface Enhanced Raman Spectroscopy 11

1.3 Computational Methods 12

1.3.1 Background 12

1.3.2 Computational Methods 13

1.4 References 14

2 Vibrational Spectroscopy of *N*-Methyliminodiacetic Acid (MIDA)-Protected Boronate Ester: Examination of the B-N Dative Bond 16

2.1 Introduction 16

2.2 Experimental and Theoretical Methods 21

2.2.1 Spectroscopic Methods 21

2.2.2 Theoretical Methods 22

2.3 Results 22

2.3.1 Spectroscopic Results 22

2.3.2 SERS Results 24

2.3.3 Theoretical Results 26

2.4 Discussion 27

2.5 Conclusions 31

2.6 References 32

3 Elucidation of the B-P Dative Bond Stretching Frequency 37

3.1 Introduction 37

3.2 Spectroscopic Methods 41

3.3 Theoretical Methods 42

3.4 Results and Discussion 43

3.5 Conclusions 49

3.6 References 50

Curriculum Vitae 52

1 Introduction

1.1 Dative Bonding and Applications

"There is nothing more fundamental to chemistry than the chemical bond."

– Roald Hoffman, Chemistry Nobel Laureate, Cornell University

There are many types of bonding in general chemistry. Ionic bonds occur due to the electrostatic attraction between two oppositely charged ions. These are generally formed between cations, which are usually metals, and anions, usually non-metals. Covalent bonds occur when two atoms share electron pairs, which are generally formed between non-metals. Metallic bonds are formed from the electrostatic attraction between a sea of delocalized electrons and positively charged metal ions. Dative bonds, or coordinative bonds, are covalent bonds where one atom provides both of the electrons in the shared pair. An example would be the bond between ammonia and hydrogen in the ammonium ion. The lone pair, or non-bonding pair, on the nitrogen of ammonia is shared with the hydrogen ion to form the ammonium ion.[1]

Dative bonded molecules have been of great interest to chemists for many years. In particular, boron forms dative bonds because of its electron deficiency. It has three pairs of electrons in its bonding level, while there is room for four pairs. This tendency can be predicted by simply looking at boron's location on the periodic table. The boronate group ($-BX_3$) acts as a Lewis acid, and some molecule acting as the Lewis base,

namely some derivative of nitrogen (-NX_3) or phosphorus (-PX_3), can donate a lone pair of electrons. The product is the Lewis adduct ($X_3N \rightarrow BX_3$), and the bond between boron and nitrogen is called a dative bond. The boron-nitrogen dative bond is widely used in synthetic applications, such as in building blocks that are precursors for generalizing and simplifying the synthesis for larger molecules. It has also been studied in applications for hydrogen storage and release. There has been a great controversy over the physical properties of the boron-nitrogen dative bond over many years, with vibrational assignments of its stretching frequency ranging from 600 – 1200 cm^{-1}. The research presented here has been performed in an attempt to elucidate the boron-nitrogen dative bond stretching frequency in *N*-methyliminodiacetic acid (MIDA) esters using infrared, Raman, and SERS spectroscopic methods in conjunction with electronic structure calculations. Even though in large molecules the boron-nitrogen stretching frequency is expected to be coupled with other modes in the molecule, the stretching frequency in methylboronic acid MIDA ester is very localized, falling in the range of 560 – 650 cm^{-1}.[2]

To further the study of dative bond stretching frequencies, boron-phosphorus (B-P) dative bonds are also investigated. Many studies have been performed on B-P dative bond containing molecules using a variety of experimental and theoretical methods over the last forty years. However, understanding the properties of the B-P dative bond stretching frequency continues to be a challenge. While B-N dative bonds are relatively well understood, a trend between the physical properties and the molecule's structure with boron-phosphorus bonds has not been determined. In order to elucidate this trend, three commercially available molecules, di(*tert*-butyl)phosphine borane, diphenylphosphine borane, and triphenylphosphine borane were studied with Raman

spectroscopy and electronic structure calculations because they have not been studied experimentally or theoretically. In addition, sixteen additional B-P containing molecules are studied theoretically. Researchers in the fields of synthetic chemistry, energy efficiency, and computational physical chemistry would find these results helpful. A trend describing the physical properties of these dative bonds would lead to better predictions and therefore better understanding for specific applications in each field.

1.2 Spectroscopic Methods

1.2.1 Vibrational Spectroscopy

Spectroscopy is the study of the interaction of light and matter. The study of this interaction can reveal a variety of intrinsic chemical and physical properties of the system being evaluated. Vibrational spectroscopy is an especially useful method in identifying the physical properties of a molecule, and it is essential to the data analysis performed in this thesis. A molecular vibration, apart from its zero point energy, can occur when atoms in a molecule are in a periodic motion. For a molecular vibration to occur, a photon with an energy exactly matching that of a vibrational energy level transition is absorbed by the atom or molecule. This absorption promotes the system to a higher energy level, causing the vibration.[4,5]

All areas of optical spectroscopy have selection rules that control what type of transitions are allowed to occur. Different types of transitions are illustrated in Figure

1.1. To generally express transitions between states, the transition dipole moment integral, Equation 1.1, is used.

$$\mu_x^{mn} = \int \psi_m^*(x)\mu_x(x)\psi_n(x)dx \neq 0 \quad (1.1)$$

In Equation 1.1, x is the spatial variable, μ is the dipole moment along the electric field direction, and m and n are two different vibrational states. The dipole moment $\mu_x(x)$ is a complex vector quantity, and its direction gives the polarization of the transition. This determines how the system will interact with an electromagnetic wave of given polarization, determining the selection rules that allow for different types of spectroscopy to occur. The probability of a transition from state n to m is nonzero within the harmonic oscillator approximation only if the transition dipole moment, μ_x^{mn}, is defined as it is above.

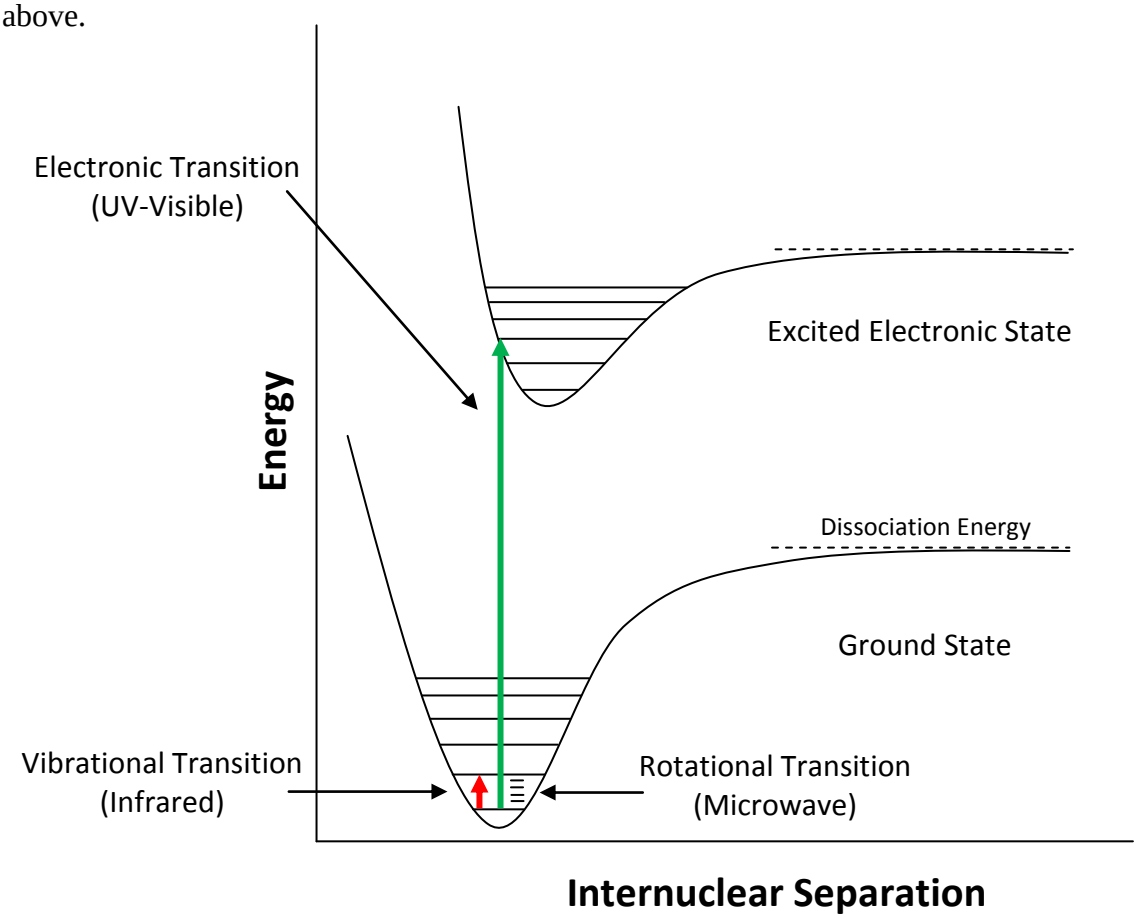

Figure 1.1 Types of transitions that can occur throughout spectroscopy.

1.2.2 The Harmonic Oscillator

A vibrational motion in a molecule can be modeled as a harmonic oscillator, which is illustrated in Figure 1.2. In classical mechanics, a harmonic oscillator can be thought of as a mass connected to a spring. The spring obeys Hooke's law, which states that the force F on the spring is directly proportional to the displacement x, as shown in Equation 1.2.

$$F = -kx \tag{1.2}$$

The position of equilibrium of the system would occur at $x = 0$. The stiffness of the spring is measured by the force constant k. The potential energy of this spring system is shown in Equation 1.3.[5]

$$V = \frac{1}{2}kx^2 \tag{1.3}$$

The harmonic potential is a parabolic equation, which implies that the force required for compression of the spring would equal extending it the same amount. This model is considered frictionless, so once the oscillator is in motion, it will remain at a constant energy.[5]

For the quantum mechanical harmonic oscillator, one considers two masses, or two atoms, connected by a spring that follows Hooke's law. Take $x = R - R_e$ as the displacement of the bond length R from its equilibrium position R_e. When solving the Schrödinger equation, $\hat{H}\Psi = E\Psi$, the Hamiltonian for this is shown in Equation 1.4.

$$\hat{H} = -\frac{\hbar^2}{2m}\frac{d^2}{dx^2} + \frac{1}{2}kx^2 \tag{1.4}$$

m is the reduced mass, and the eigenvalues of this operator are the harmonic oscillator energy levels shown in Equation 1.5.

$$E_v = \left(v + \frac{1}{2}\right) h\nu_0 \tag{1.5}$$

v is a single quantum number since this is a one-dimensional system. ν_0 is the natural frequency, Equation 1.6.[4,5]

$$\nu_0 = \frac{1}{2\pi}\sqrt{\frac{k}{m}} \tag{1.6}$$

The ground state probability density is concentrated at the origin. This means the particle spends most of its time at the bottom of the potential well. As the energy increases, the probability density becomes concentrated at the classical turning points, where the state's energy coincides with the potential energy. This is consistent with the classical harmonic oscillator, in which the particle spends most of its time at the turning points.[4,5]

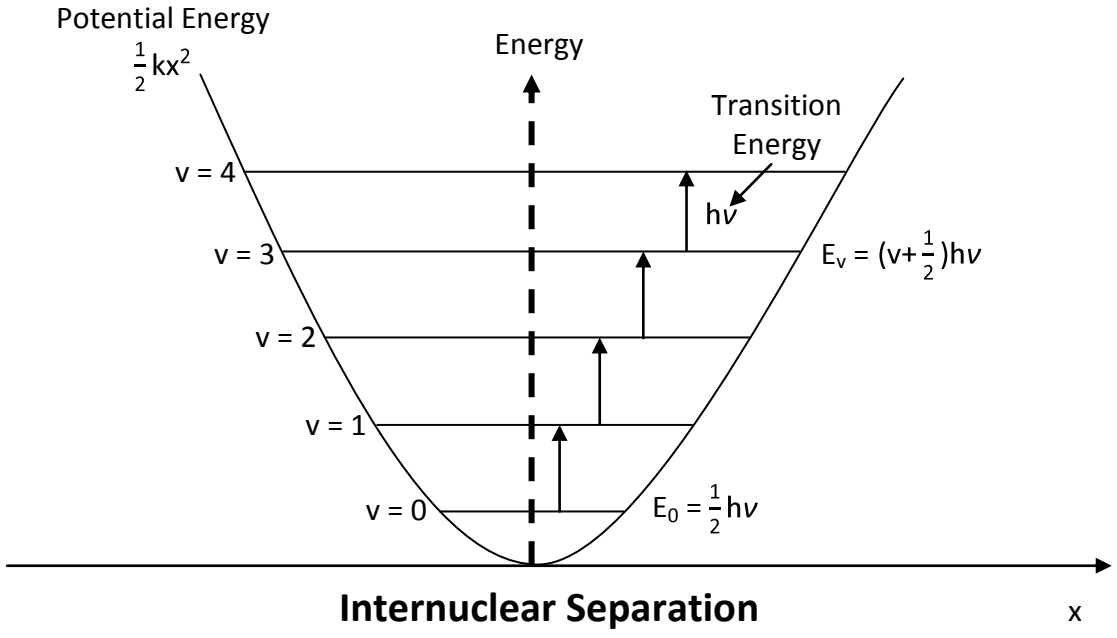

Figure 1.2 Vibrational transitions illustrated by the harmonic oscillator.

1.2.3 Normal Modes

In order to describe the individual vibrations within a molecule, vibrational coordinates must be defined. They are described by the changes in position of the atoms in the molecule. The normal coordinates of an atom are the positions of the atoms away from their equilibrium positions. Normal refers to the fact that the displacements of an atom along any two different normal modes are orthogonal, i.e. have an inner product of zero. They are determined by solving a determinant that includes a summation over the Cartesian coordinates of the atom positions. A molecule with N atoms has $3N$-6 normal modes of vibration, and a linear molecule has $3N$-5 normal modes because rotation about its molecular axis cannot be observed. This number corresponds to three degrees of freedom of motion for each atom (i.e. in the x, y, and z directions) minus the number of rotational and translational motions. Any motion of the atoms of a molecule can be represented by an equation of motion that is nothing more than a linear combination of the normal mode equations of motion. Each normal mode has an energy associated with it, although the energy may be the same for two normal modes.[4,5]

1.2.4 Raman Spectroscopy

Raman spectroscopy is used to study the vibrational and rotational modes of molecules through excitation by a monochromatic light source and measurement of the inelastic, or Raman, scattering of the light. This is known as Stokes and anti-Stokes scattering. When light, usually from a laser, interacts with a molecule, the molecule becomes excited to a virtual energy state. When the excited state relaxes, a shift in the energy of the photon

can sometimes occur, which is characteristic to a certain frequency and, therefore, vibration of the molecule.[3]

In Raman spectroscopy, the energy of the incident photons that excite the molecule and the energy of the photons that are scattered and detected are different. This type of scattering was first observed and reported by C. V. Raman in 1928 using the sun as an excitation source.[6] Here, argon and krypton ion lasers are employed to study the systems described in Chapters 2 and 3.

An introductory discussion of the relationship between the Raman Effect and molecular vibrations is presented below. The induced dipole moment in a molecule is equal to the product of the polarizability and the applied electric field. Change in polarizability leads to change in the dipole moment, making the transition dipole moment (Equation 1.1) nonzero. Molecules are constantly vibrating at any temperature above 0 K. For a homonuclear diatomic molecule, we can write the nuclear displacement from the equilibrium position as Equation 1.7.[4,5]

$$q = q_0 \cos\omega_v t \tag{1.7}$$

Equation 1.7 is a result of the harmonic oscillator model described above. These vibrations cause a change in electron density, and as a result, the polarizability is not accurately represented by a static variable but as a function of nuclear position (Equation 1.8).

$$\alpha = \alpha_0 + \frac{\partial \alpha}{\partial q_0} q_0 + \cdots \tag{1.8}$$

This series can be truncated at the term linear in q_0 for small amplitudes of vibration. Now, Equation 1.8 can be substituted into an equation for an oscillating dipole to give Equation 1.9.

$$p = \alpha_0 \mathrm{E}_0 \cos\omega t + \frac{\partial \alpha}{\partial q_0} q \mathrm{E}_0 \cos\omega t \quad (1.9)$$

Next, Equation 1.7 is substituted into 1.9 to yield 1.10.

$$p = \alpha_0 \mathrm{E}_0 \cos\omega t + \frac{\partial \alpha}{\partial q_0} q \mathrm{E}_0 \cos\omega t \cos\omega_v t \quad (1.10)$$

Lastly, applying a trigonometric identity, we obtain a classical theory describing Raman scattered light.

$$p = \alpha_0 \mathrm{E}_0 \cos\omega t + \frac{1}{2}\frac{\partial \alpha}{\partial q_0} q \mathrm{E}_0 \{\cos[(\omega + \omega_v)t] + \cos[(\omega - \omega_v)t]\} \quad (1.11)$$

The above equation shows that the dipole, *p*, induced by light interacting with the vibrating diatomic molecule is oscillating with frequency ω. Also, the dipole contains components oscillating with frequencies $\omega + \omega_v$ and $\omega - \omega_v$. The result is that the induced dipole is emitting light with frequencies greater than or less than the incident light by an amount equal to the frequency of vibration.[4,5]

There are three energy levels and transition frequencies involved in Raman spectroscopy, as illustrated in Figure 1.3. First, when the energy of the final vibrational state, after excitation to a virtual state, is higher than that of the initial state, it is known as Stokes scattering. Also, when the energy of the final state, after excitation to a virtual state, is lower than that of the initial state, it is known as anti-Stokes scattering. In Stokes scattering, the wavelength of the photon released is higher than that of the exciting photon, and the reverse is true for the anti-Stokes scattering. The third transition that occurs is when a molecule is excited to a virtual state and then returns to its original state, which is elastic, or Rayleigh, scattering. When Rayleigh scattering occurs, the photons that are detected from the molecules have the same wavelength as the photons that are used to initially excite the molecule (ω in Equation 1.10). Detection is limited to Stokes

and anti-Stokes scattering since Rayleigh scattered photons have the same wavelength as the incident photons.[3,5]

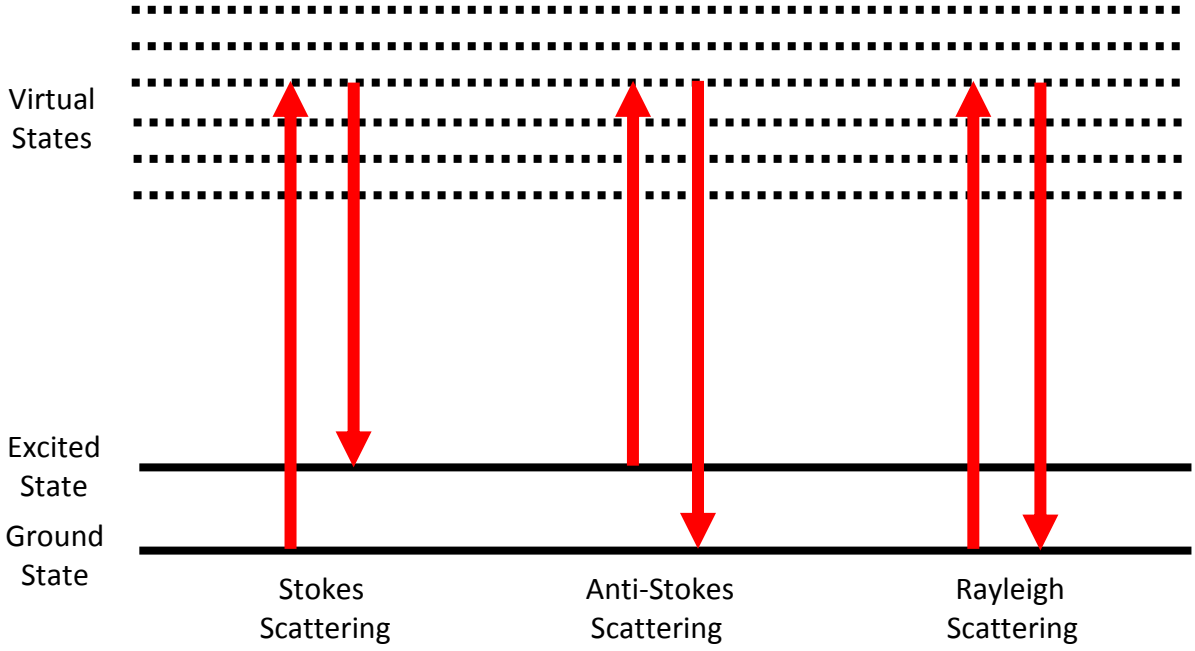

Figure 1.3 Raman energy transitions.

Since the intensity of a scattered photon from the Raman effect is very weak (probability of one in a million for inelastic scattering), a strong excitation source must be used. Also, because the probability of the anti-Stokes scattered photons is significantly less than the Stokes scattered photons (one in a billion), the Stokes scattered photons are usually the ones that are detected for measurement.[3]

The predicted energy for a normal mode, as described in section 1.3, is employed to assign the peaks in a Raman spectrum to particular normal modes. However, not every normal mode will have a peak present in the Raman spectrum. Certain normal modes are not Raman active. If the derivative of polarizability in Equation 1.11 is zero, the dipole will not have components oscillating at either of the Raman shifted frequencies.

Therefore, no Raman scattered light will appear. Physically, we interpret this change in polarization with a normal mode being a requirement for that mode's Raman activity, which was previously discussed with the transition dipole integral (see Equation 1.1). This means that if a molecule is fully symmetrical, it will be Raman active but not infrared (IR) active, due to the change in polarizability, but not its dipole moment. A change in the dipole moment leads to IR activity. Thus, Raman and IR spectroscopy are complementary vibrational spectroscopy tools widely used to determine the physical properties of various molecular systems.[4,5]

1.2.5 Surface Enhanced Raman Spectroscopy

Surface enhanced Raman spectroscopy (SERS) is a spectroscopic technique that enhances Raman signal by adsorbing a molecule on a SERS active substrate. A good example of such a substrate is a roughened metal surface. SERS can enhance Raman signal as much as 10^{11} times. The increase in intensity of the Raman signal occurs because of an enhancement in the electric field provided by the surface's atomic structure. The electromagnetic field of the excitation radiation is incident on the sample, which is the case for normal Raman scattering. In SERS, the roughened surface provides another electromagnetic field, that of the metal particle. These two fields are very close as the sample is adsorbed on the roughened surface. Because of this, any electromagnetic field from the particle will contribute a large factor to the total coupled electromagnetic field. The intensity of Raman signal is proportional to the square of the total electromagnetic field; thus, the magnitude of the electromagnetic field of the particle is

crucial to the intensity of Raman signal. The resulting electromagnetic field is very intense, leading to the requirement of the roughened surface for SERS to be successful.[7]

In some systems, the electromagnetic theory behind enhancement does not fully explain the magnitude of the enhancement observed. For many molecules, especially with a lone pair of electrons, a chemical mechanism can occur that involves charge transfer between the chemisorbed species and the metal surface. The chemical mechanism only applies in specific cases and probably occurs along with the electromagnetic mechanism.[8]

1.3 Computational Methods

1.3.1 Background

"The underlying physical laws necessary for the mathematical theory of a large part of physics and the whole of chemistry are thus completely known, and the difficulty is only that the exact application of these laws leads to equilibrium much too complicated to be solvable." – P. A. M. Dirac, Nobel Laureate

Computational chemistry is an important field of chemistry in which calculations based on quantum mechanics can be utilized to explain experimental results. These calculations are based on the Schrödinger equation, Equation 1.11. However, it can only be solved exactly for a one-electron system. Because of this, various numerical methods are employed for approximating wave functions and intrinsic properties, such as energy.

$$\hat{H}\Psi = E\Psi \tag{1.11}$$

In the equation, *E* is the total energy of the system. Ψ is the *n*-electron wave function that depends both on the identities and positions of the nuclei and the total number of electrons. $\hat{H}$ is the Hamiltonian operator, Equation 1.12, that specifies the kinetic and potential energies for each of the particles.[4,5]

$$\hat{H} = -\frac{\hbar^2}{2m_e}\sum_{i}^{electrons}\nabla_i^2 - \frac{\hbar^2}{2}\sum_{A}^{nuclei}\frac{1}{M_A}\nabla_A^2 - \frac{e^2}{4\pi\varepsilon_0}\sum_{i}^{electrons}\sum_{A}^{nuclei}\frac{Z_A}{r_{iA}} + \frac{e^2}{4\pi\varepsilon_0}\sum_{i}^{electrons}\sum_{j}^{electrons}\frac{1}{r_{ij}} + \frac{e^2}{4\pi\varepsilon_0}\sum_{A}^{nuclei}\sum_{B}^{nuclei}\frac{Z_A Z_b}{R_{AB}} \quad (1.12)$$

In this equation, Z_A is nuclear charge, M_A is the mass of nucleus *A*, m_e is the mass of electron, R_{AB} is the distance between nuclei *A* and *B*, r_{ij} is the distance between electrons *i* and *j*, r_{iA} is the distance between electron *i* and nucleus *A*, ε_0 is the permittivity of free space, $\hbar$ is the Planck constant divided by 2π, and ∇_i^2 is the Laplace operator of particle *i*. Computational methods involve solving the Schrödinger equation using a variety of approximations.

1.3.2 Computational Methods

Various computational methods are employed in the research presented in this thesis. B3LYP density functional[10,11], MP2[9], and M06-2X global hybrid density functional[12] methods are used to evaluate the different dative bonded systems. Each method and basis set combination gives quite different results when compared to experimental values. While various basis set sizes were used, the large triple zeta basis set, 6-311G(2*df*,2*pd*),

yielded the best results in this study. As expected, when the basis set quality increases, the closer the computational results are to the experimental results. For the dative bond stretching region, B3LYP tends to underestimate the vibrational energy while MP2 tends to overestimate. M06-2X is a fairly new method that has proven to predict dative bonds well, so it was also employed in this study for comparison.[12] The INTDER2005 program[13] was also employed to determine the total energy distributions (TEDs) characterizing the normal modes of each dative bonded system. The results of these comparisons are presented in Chapters 2 and 3.

1.4 References

(1) Tro, N. J.; *Chemistry: A Molecular Approach*, **2008**.

(2) D. N. Reinemann, A. M. Wright, J. D. Wolfe, G. S. Tschumper, and N. I. Hammer, *Journal of Physical Chemistry A*, 115, 6426-6431, **2011**.

(3) Garland, C. W.; Nibler, J.W.; *Experiments in PhysicalChemistry*, **2009**.

(4) Engel, T.; Reid, P. *Physical Chemistry*, **2010**.

(5) McHale, J. L. *Molecular Spectroscopy*, **1999**.

(6) Raman, C.V., *Nature*, **1928**.

(7) Smith, E.; Dent, G., *Modern Raman Spectroscopy: A Practical Approach*, **2005**.

(8) Lombardi, J.R.; Birke, R.L., *Journal of Physical Chemistry*, **2008**.

(9) Møller, C.; Plesset, M. S. *Phys. Rev.* **1934**, 46, 618.

(10) Becke, A. *J. Chem. Phys.***1993**, 98, 5648.

(11) Lee, C.; Yang, W.; Parr, R. G. *Phys. Rev. B***1988**, 37, 785.

(12) Zhao, Y.; Truhlar, D. G. *Theor. Chem. Acc.***2008**, 120, 215.

(13) INTDER2005 is a general program developed by Wesley D. Allen and co-workers that performs various vibrational analyses and higher-order nonlinear transformations among force field representations.

2 Vibrational Spectroscopy of *N*-Methyliminodiacetic Acid (MIDA)-Protected Boronate Ester: Examination of the B-N Dative Bond

2.1 Introduction

The formation of many important biological polymers and macromolecules, as well as various synthetic materials, relies on iterative coupling of preassembled building blocks. The purpose of having these building blocks is to generalize and simplify the various methods of syntheses of large molecules.[1] These processes are efficient and flexible, whereas the syntheses of smaller molecules are much more involved. A solution to the difficulty involved in synthesizing these smaller molecules is to employ boronic acids. Boronic acids are indeed very useful building blocks for organic syntheses.[2] For example, the Suzuki Miyaura reaction between an organohalide and a boronic acid is a powerful tool in generalizing the method for C-C bond formation in the synthesis of complex molecules. An underlying problem, however, involves reaction scheme incompatibilities between most synthetic reagents. An often employed solution to this incompatibility is to use boronic ester counterparts. These are more compatible with many synthetic schemes, although liberation of the boronic acid requires harsh conditions that interfere with the synthetic substrates.

Burke and co-workers recently developed a new class of molecules that allow for milder reaction conditions. This was accomplished through complexation of the boronic acid with a trivalent ligand, *N*-methyliminodiacetic acid (MIDA).[1-3] This rehybridizes the boron center to sp^3, dramatically increasing the stability of the boronic acid and allowing

for the synthesis of complex molecules to take place. The MIDA esters are unreactive under anhydrous cross-coupling conditions, are stable in air, and can be deprotected easily using mild aqueous basic conditions. This new molecular class serves as the first general solution where both benchtop stability and the capacity for in situ slow release of the boronic acids is included.[1-3] The key to the success of these molecules as synthetic reagents is the B-N dative bond. The stability of the MIDA esters also makes them ideal candidates for studying B-N dative bonds spectroscopically. Here, we compare experimental infrared, Raman, and surface enhanced Raman spectroscopy (SERS) spectra of methylboronic acid (MBA) MIDA ester (structure shown in Figure 2.1) to theoretical predictions in an effort to describe the physical properties of the B-N dative bond contained in this molecule.

Ammonia borane and trimethylamine borane (structures shown in Figure 2.1) are simple prototypes that have been studied extensively to investigate dative B-N bonding interactions.[4-51] Throughout the years, there have been many different attempts to assign the B-N dative bond stretching frequency in these and similar molecules. In 1957, Rice and co-workers experimentally recorded Raman and infrared spectra of liquid trimethylamine borane and assigned the B-N stretching motion to a peak at 1255 cm^{-1}.[5] A year later, Taylor et al. pointed out that the few already recorded spectra of amine boranes had an unexpectedly high value for the B-N stretch.[6] For example, this motion in species such as BF_3NH_3,[52] $C_5H_5NBF_3$,[53] $H_3NB(CH_3)_3$,[54] and $(CH_3)_3NBH_3$[5] had been previously assigned to between 980 and 1255 cm^{-1}. These authors asserted that the stretching frequency should be much lower in energy. As a result, they assigned the B-N stretch in trimethylamine borane to 667 and in ammonia borane to 785 cm^{-1}.[6,8] In 1965,

Sawodny et al. measured the vibrational spectrum of ammonia borane (BH_3NH_3) in the solid state and assigned the B-N stretch at 776 cm^{-1}.[9] Odom and co-workers realized in 1974 that the B-N stretch of trimethylamine borane should be in the same spectral

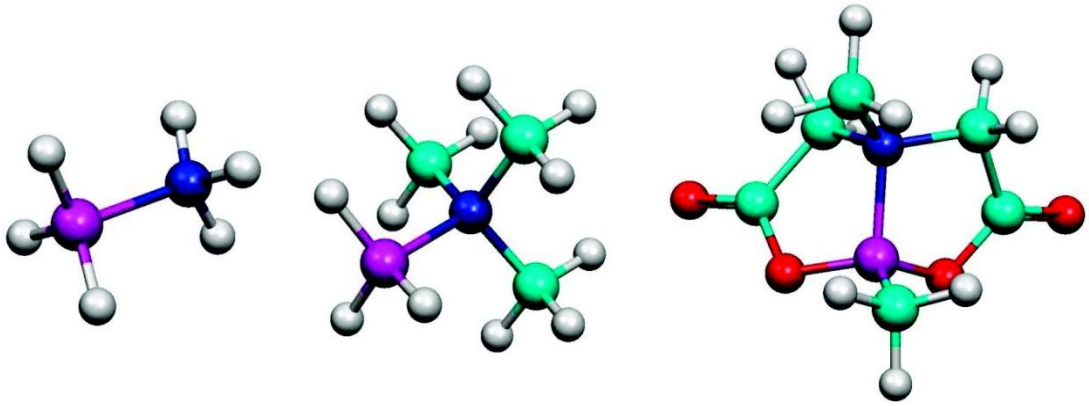

Figure 2.1 Molecules that contain a B-N dative bond: ammonia borane (left), trimethylamine borane (middle), and methylboronic acid MIDA ester (right).

window as C-N stretches. Together with the low intensity of this normal mode in infrared spectra, confusion with the assignment of this vibration in earlier studies is not surprising.[13] Odom suggested that Raman spectroscopy is likely a better method than infrared to observe B-N stretching modes, and the authors reassigned the B-N stretch in trimethylamine borane to 660 cm^{-1}.

In 1995, Vijay and co-workers performed a theoretical study on ammonia borane using various basis sets and levels of theory to ascertain which level of theory best agreed with the already available experimental spectra.[23] The authors utilized Taylor's assignment of the B-N stretch at 785 cm^{-1} as the experimental value to which they compared.[6,8] They suggested that the SCF method, which predicted a B-N stretch between 617 and 625 cm^{-1}, underestimated experimental observations and could not

accurately describe the B-N bond in ammonia borane, even with extended basis sets. At the MP2 level, which predicted the B-N stretch between 678 and 690 cm^{-1}, the use of larger basis sets with more diffuse functions also did not improve the agreement between experiment and theory with regard to the location of the B-N stretching frequency. Calculations performed using the QCISD method lowered the energy of the B-N stretching motion by 13 cm^{-1} compared to MP2, but the authors recommended the use of the CCSD(T) coupled cluster method with large basis sets, which they could not perform at the time due to disk space limitations.

Dillen et al. in 2003 attempted to conclusively assign the B-N stretching frequency of solid ammonia borane and end the controversy observed in the previous decades.[31] The authors assigned the energy of the B-N stretching motion, which is effectively localized on an individual BH_3NH_3, to a gas phase calculated value of 610 cm^{-1}. To model the crystalline environment of BH_3NH_3 in the solid state, the authors computed MP2/6-31G(d) vibrational frequencies of a BH_3NH_3 molecule surrounded by its 8 nearest neighbors fixed at their positions from the crystal structure. HF/6-31G(d) vibrational frequencies were also computed for models containing as many 30 neighboring ammonia borane molecules. The computed B-N stretching frequencies of these BH_3NH_3 clusters were compared to the previous experimental values, and the authors noted that Smith's value of 968 cm^{-1} seemed very unlikely. However, the molecular cluster computational results were consistent with Taylor's earlier experimental assignment of 785 cm^{-1} in the solid state. Ammonia borane is perhaps not the best dative bond containing candidate to study, however, due to intermolecular dihydrogen bonding between adjacent molecules in the solid state.[55,56] Dillen et al.

pointed out that these intermolecular interactions and the accompanying dramatic shortening of the B-N bond in the solid state produce a blue shift of over 100 cm^{-1}.[31]

Computational studies of amine-boranes by Gilbert in 2004,[34] LeTourneau et al. in 2005,[39] and Plumley and Evanseck in 2007[47] demonstrated that the B3LYP[57,58] hybrid density functional tends to overestimate the lengths and significantly underestimates the dissociation energies/enthalpies of coordinate covalent B-N bonds. Consequently, B3LYP cannot be expected to provide reasonable vibrational frequencies of the title compound, in the B-N stretching region. In contrast, the global hybrid density functional M06-2X[59] has been shown to provide a far more reliable description of B-N dative bonds.[60,61] In fact, comparison to experimental data as well as results from CCSD(T) and QCISD(T) computations indicates that M06-2X even outperforms second-order Møller-Plesset perturbation theory (MP2)[62] for these systems.

Here, we present experimental vibrational spectra of MBA MIDA ester using a variety of vibrational spectroscopic methods. Compared to the simpler B-N containing molecules, ammonia borane and trimethylamine borane, MBA MIDA ester is much larger, and the sp^3 hybridized boron atom is secured by two five-membered rings, making it stable for spectroscopic study. We compare our experimental spectra with the results of ab initio calculations using both the MP2 and M06-2X methods and different sized basis sets to assign the location of the B-N stretching frequency of the dative bond in MBA MIDA ester.

2.2 Experimental and Theoretical Methods

2.2.1 Spectroscopic Methods

Methylboronic acid MIDA ester was obtained from Sigma-Aldrich and was used for the Raman, SERS, and infrared experiments presented here without any further purification. Raman spectra of MBA MIDA ester were obtained using 514.5 and 676.4 nm laser lines from argon or krypton ion lasers. A Ramanor HG2-S Raman scanning spectrometer was employed to acquire Raman spectra using the 514.5 nm line from an Ar ion laser. A Nachet NS 400 micro-Raman setup was used to analyze the sample with an incident laser power of 300 mW at the sample, and a 0.5 cm^{-1}/s scan speed was employed over the range 0-4000 cm^{-1}. Spectra were acquired and interpreted using a custom computer program written using National Instruments LabView. A Jobin-Yvon T64000 Raman spectrometer with CCD detection was used to acquire Raman spectra using the 676.4 nm line from a Kr ion laser. Infrared spectra were acquired in a salt pellet using a Bruker IFS66 spectrometer with 1024 scans with 1 cm^{-1} resolution. The SERS substrates created to study MBA MIDA esters were fabricated using a vacuum deposition chamber. Pressures in the deposition chamber were approximately 1 x 10^{-6} Torr throughout the deposition process. Glass slides were cleaned and then coated with silver island films to 7 nm at a deposition rate of 0.02 nm/s. MBA MIDA ester was deposited on the SERS active substrates from solutions in various solvents via the drop method. SERS spectra were acquired using the 514.5 nm line from a Coherent Innova Ar ion laser providing approximately 300 mW of power at the sample. The microRaman setup described above was used to collect and analyze the scattered light.

2.2.2 Theoretical Methods

The Gaussian 09[63] software package was employed to optimize the structure and to calculate the unscaled harmonic vibrational frequencies as well as the corresponding Raman and infrared intensities of MBA MIDA ester. The M06-2X global hybrid density functional[59] and second-order Møller-Plesset perturbation theory (MP2)[62] were used in conjunction with two split-valence basis sets, 6-31G(*d*,*p*) and6-311G(*2df*,*2pd*). Harmonic vibrational frequencies confirmed that the optimized geometry corresponds to a true minimum on the potential energy surface associated with each combination of method and basis set. Default convergence criteria and frozen core conventions were employed in each calculation. Simulated spectra were created by combining Lorentzians for each normal mode using a custom program developed with National Instruments LabView. The INTDER2005 program[64] was employed to determine the total energy distributions (TEDs) characterizing the normal modes. The B-N stretch is defined as the simple internal coordinate S1 = r(B-N).

2.3 Results

2.3.1 Spectroscopic Results

Infrared and Raman spectra of MBA MIDA ester are presented in Figure 4.2. Raman spectra acquired using the 514.5 nm Ar ion laser line exhibited a very large, polynomial-shaped background. In 2007, Zhao et al. proposed a solution for eliminating the fluorescence background common in Raman spectra by implementing an automated background subtraction algorithm employed while Raman spectra were being collected.[65]

Following that suggestion, we fitted a polynomial to the baseline of the raw spectra and subtracted it. The resulting spectrum for the 514.5 nm excitation (shown in Figure 2.2) represents the sum of on average 20 individual scans, displays a relatively flat baseline, and agrees well with the spectra obtained using the Kr ion 676.4 nm laser line.

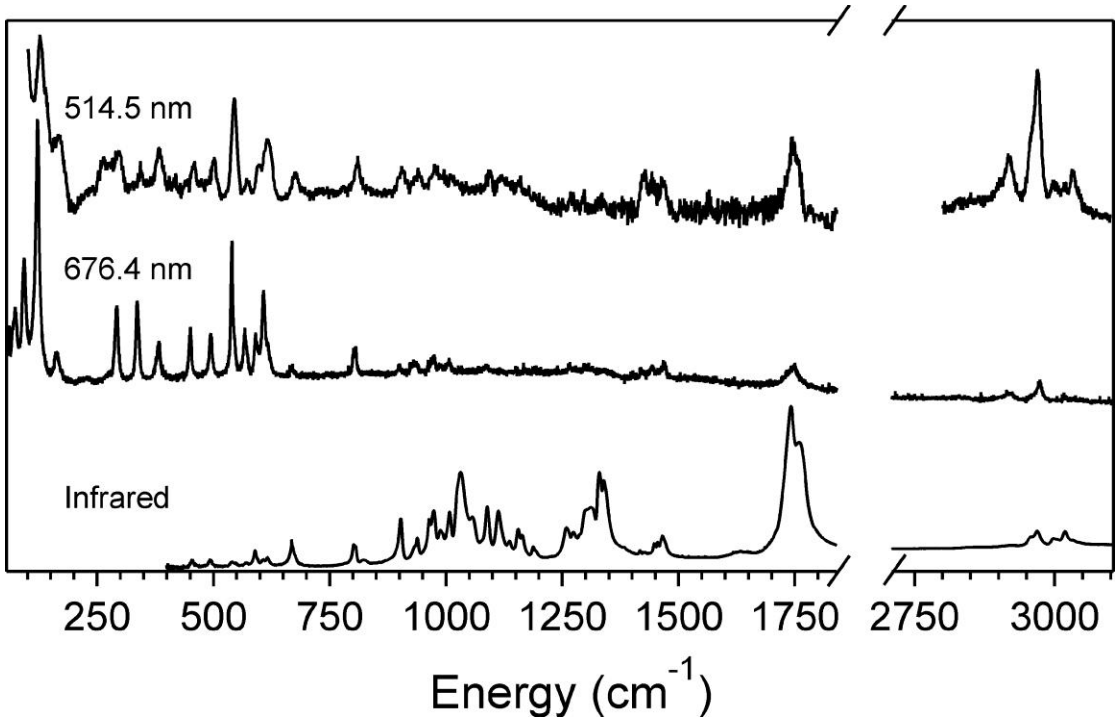

Figure 2.2 Infrared spectrum (bottom) and Raman spectra of methylboronic acid MIDA ester using 676.4 nm (middle) and 514.5 nm (top) laser excitation.

Interestingly, spectra acquired using the Kr ion 647.1 nm laser line (not shown) also exhibited a large polynomial-shaped background. It is observed that the positions of the peaks in the Raman and infrared experimental spectra agree closely with one another. However, at the lower energy end of the spectrum, the vibrational modes in the Raman spectra are relatively more pronounced than they are in the infrared spectrum. This is consistent with the earlier observations by Odom and co-workers in the case of

trimethylamine borane.[13] The opposite is true in the central part of the spectra where peaks in the infrared spectrum are more prominent than in the Raman. The carbonyl stretches at 1700 cm^{-1} correlate well with one another in both Raman and infrared, appearing as a doublet, as do the location of the C-H stretches. The carbonyl stretching region represents the most intense features in the infrared spectrum. The C-H stretches at 2900-3050 cm^{-1} have a greater intensity in the 514.5 nm excited Raman spectrum than in the 676.4 nm Raman or infrared spectra. Also, there are additional peaks evident in the Raman spectrum using 514.5 nm excitation that are not observed when 676.4 nm is employed.

2.3.2 SERS Results

Surface-Enhanced Raman Spectroscopy (SERS) was employed for enhancing the Raman peaks in the spectrum of MBA MIDA ester and to explore possible interactions with a silver substrate. It was observed that the choice of solvent had a great effect on the resulting SERS spectrum.[66] For example, SERS spectra acquired using varying concentrations of MBA MIDA ester in methanol showed no significant peaks. Results using acetone were much more pronounced and are shown in Figure 2.3. The prominent peaks in the SERS spectrum indicate that the apparent fluorescence background has been quenched to some extent. However, the SERS continuum, the sloping baseline present in many SERS spectra, is evident in the spectrum presented here. Recent studies suggest that this continuum may be of physical importance, arising from surface enhanced fluorescence.[67,68] The peaks in Figure 2.3, using the 676.4 nm laser line, correlate well

with the peaks in the SERS spectrum, suggesting that MBA MIDA ester was likely physisorbed to the SERS substrate. Visible exceptions include the broad feature observed at 1000 cm^{-1} and a prominent peak at 1126 cm^{-1}, which is marked with an asterisk. The prominence of these features suggests an intimate interaction between MBA MIDA ester and the silver substrate. By comparison with theoretical predictions, most peaks in this region of the vibrational spectrum correlate to motion of the nitrogen atom and its three neighboring CH_n groups. The intensity of this peak may point to an interaction between the nitrogen atom and silver atoms in the substrate in some of the MBA MIDA ester molecules.[69-71]

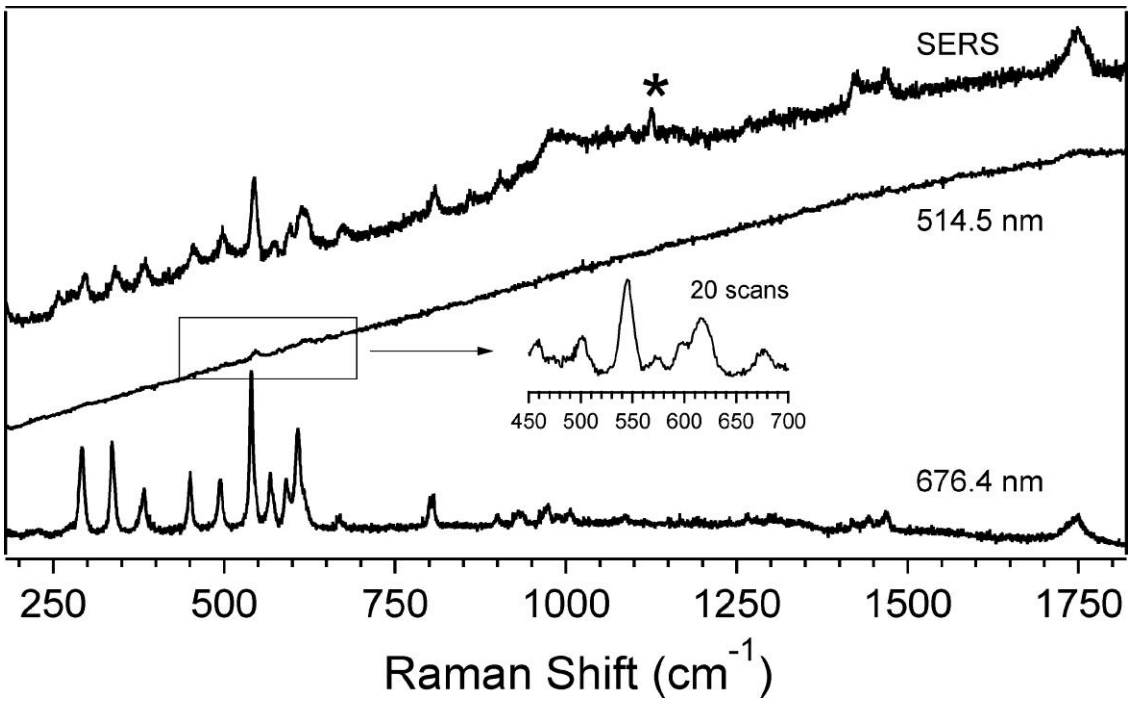

Figure 2.3 Comparison of a SERS spectra of methylboronic acid MIDA ester in acetone (top), nascent Raman spectrum using 514.5 nm (middle), and 676.4 nm (bottom) excitation, respectively.

2.3.3 Theoretical Results

To aid in the characterization of normal modes in the experimental spectra and to help characterize the structure of MBA MIDA ester, quantum chemistry computations were performed using a variety of method and basis set combinations. The B-N bond lengths are listed in Table 2.1 for each level of theory. For a given basis set, the MP2 and M06-2X bond lengths differ by only 0.02 Å. Harmonic vibrational frequencies were also computed, and analysis of the corresponding TEDs reveals that only one mode has significant B-N stretching character (simple internal coordinate S_1). These vibrational frequencies are also provided in Table 2.1 along with the percent B-N stretching character. At the MP2/6-311G(*2df,2pd*) level of theory, for example, the mode at 601 cm^{-1} is 62% B-N stretch, while no other mode has more than 14% B-N stretching character. Similar results are obtained for the MP2/6-31G(*d,p*) and M06-2X/6-311G(*2df,2pd*) vibrational frequencies. Only with the small basis set and the M06-2X functional does another vibrational mode have more than 16% B-N stretching character.

Method	Basis	r(B-N)	ω	%S_1
MP2	6-31G(*d,p*)	1.67	602	65
MP2	6-311G(*2df,2pd*)	1.66	601	62
M06-2X	6-31G(*d,p*)	1.69	577	42
M06-2X	6-311G(*2df,2pd*)	1.68	579	71

Table 2.1 B-N Bond Length (Å) and Vibrational Frequencies (cm^{-1}) of the Mode with the Largest Percentage of B-N Stretching Character (Simple Internal Coordinate S_1)

2.4 Discussion

There has been great controversy over the assignment of B-N stretching frequencies in the past. Reasons for this disagreement include the instability of the molecules studied and the poor correlation between theoretical methods and earlier experiments. Shown in Figure 2.4 is a comparison of the Raman spectrum of MBA MIDA ester in the range 50-1900 cm^{-1} with unscaled results at the MP2/6-311G(*2df,2pd*) and M06-2X/6-311G(*2df,2pd*) levels of theory. Frequencies were calculated using both isotopes of boron and weighted using the appropriate natural abundances. With two isotopes having significant natural abundances (80.1% ^{11}B and 19.9% ^{10}B), peaks involving motion of the central boron atom are broadened, yielding as light shoulder.

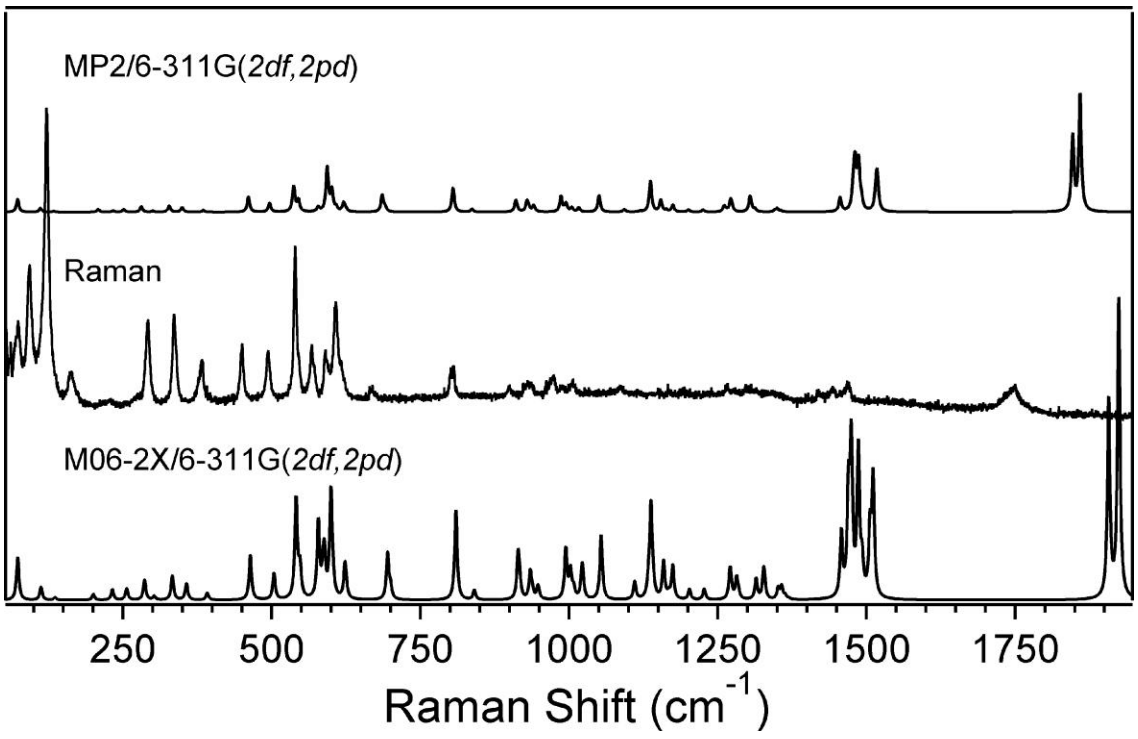

Figure 2.4 Comparison of experimental (676.4 nm excitation) and theoretical Raman spectra.

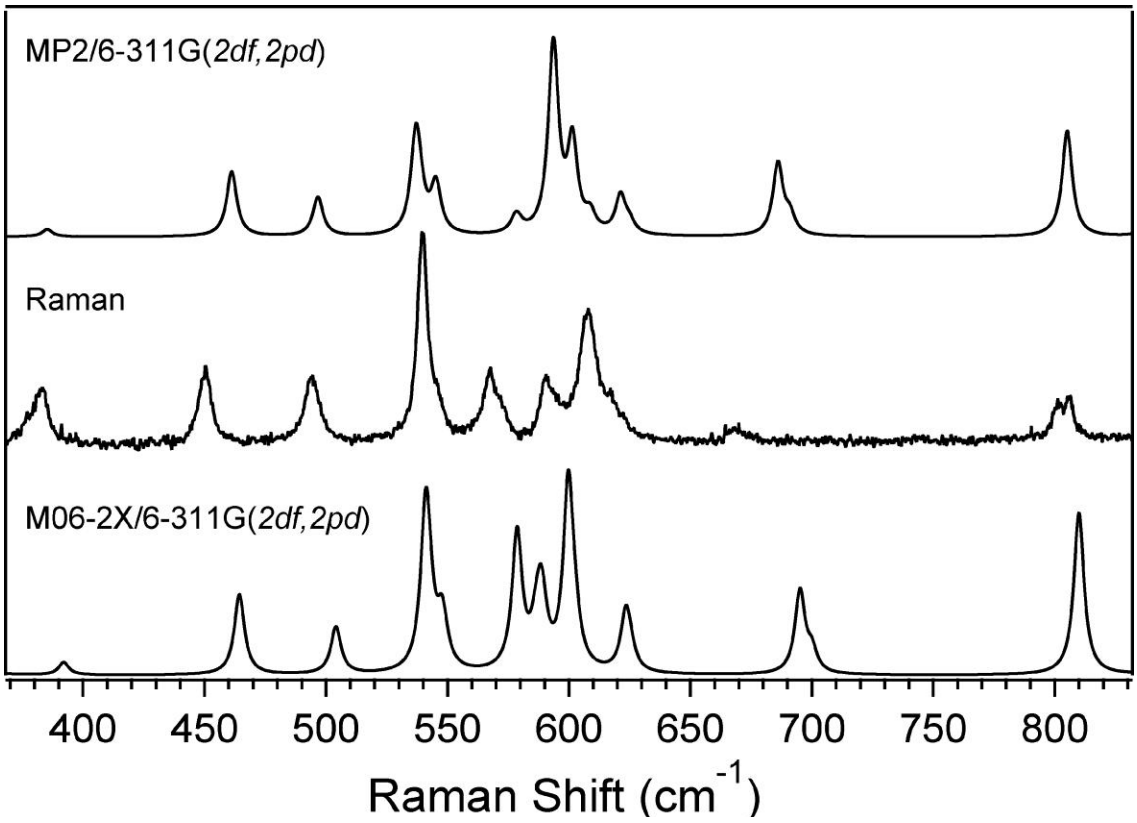

Figure 2.5 Detailed comparison of experimental (676.4 nm excitation) and theoretical Raman spectra.

Figures 2.5 and 2.6 show a detailed comparison between experiment and theory in the region associated with B-N stretching. Agreement between experiment and theory is quite good for most peaks, as is the agreement between the MP2 and M06-2X results. Significant coupling of simple internal coordinates is to be expected in a molecule of this size, particularly in a system with fused rings and C1 symmetry. On average, the maximum contribution to the TED of a vibrational mode from a single simple internal coordinate is 40%. The BN stretch, however, is predominantly associated with one normal vibrational mode. With the larger basis set, M06-2X predicts this mode to occur at 579 cm^{-1}, whereas MP2 predicts a higher energy of 601 cm^{-1}, and the corresponding TEDs indicate they are 71% and 62% B-N stretch (simple internal coordinate S_1),

respectively. To further put this in perspective, at the MP2/6-311G(*2df*,*2pd*) level of theory, only 7 of the 60 normal modes have a larger contribution from one simple motion. Thus, the B-N stretch in MBA MIDA ester is predicted by both methods to be quite "pure". No other vibrational mode has more than 14% and 11% B-N stretching character at the MP2/6-311G(*2df*,*2pd*) and M06-2X/6-311G(*2df*,*2pd*) levels of theory, respectively.

All of the experimentally observed peaks in Figures 2.5 and 2.6 are accounted for by both levels of theory. Both MP2 and M06-2X predict large Raman and infrared intensities for the B-N stretch, suggesting that it should be readily visible in both spectra. In the range 560-650 cm^{-1}, experimentally there are four peaks, one of which appears as a shoulder at 617 cm^{-1} in the Raman spectrum but is clearly visible in the infrared. Both MP2 and M06-2X predict four peaks in this spectral window, which accounts for all of the experimentally observed peaks. A direct comparison of the MP2/6-311G(*2df*,*2pd*) and experimental spectra suggests that the mode with the greatest B-N stretching character is likely the experimentally observed peak at 608 cm^{-1}, while M06-2X/6-311G(*2df*,*2pd*) frequencies suggest that it is the experimental peak at 568 cm^{-1}.

The close proximity of experimental peaks in this region makes it difficult to assign this mode to a specific experimental peak, but our computational results indicate that the mode with the greatest amount of B-N stretching character appears in this spectral window. Assignment to the experimental peak at 608 cm^{-1}, using the MP2 results as a guide, would yield an experimental wavenumber value that is actually higher than that for the calculated harmonic vibrational frequency. The M06-2X/6-311G(*2df*,*2pd*) results suggest the B-N stretching mode is most likely associated with the peak at 568

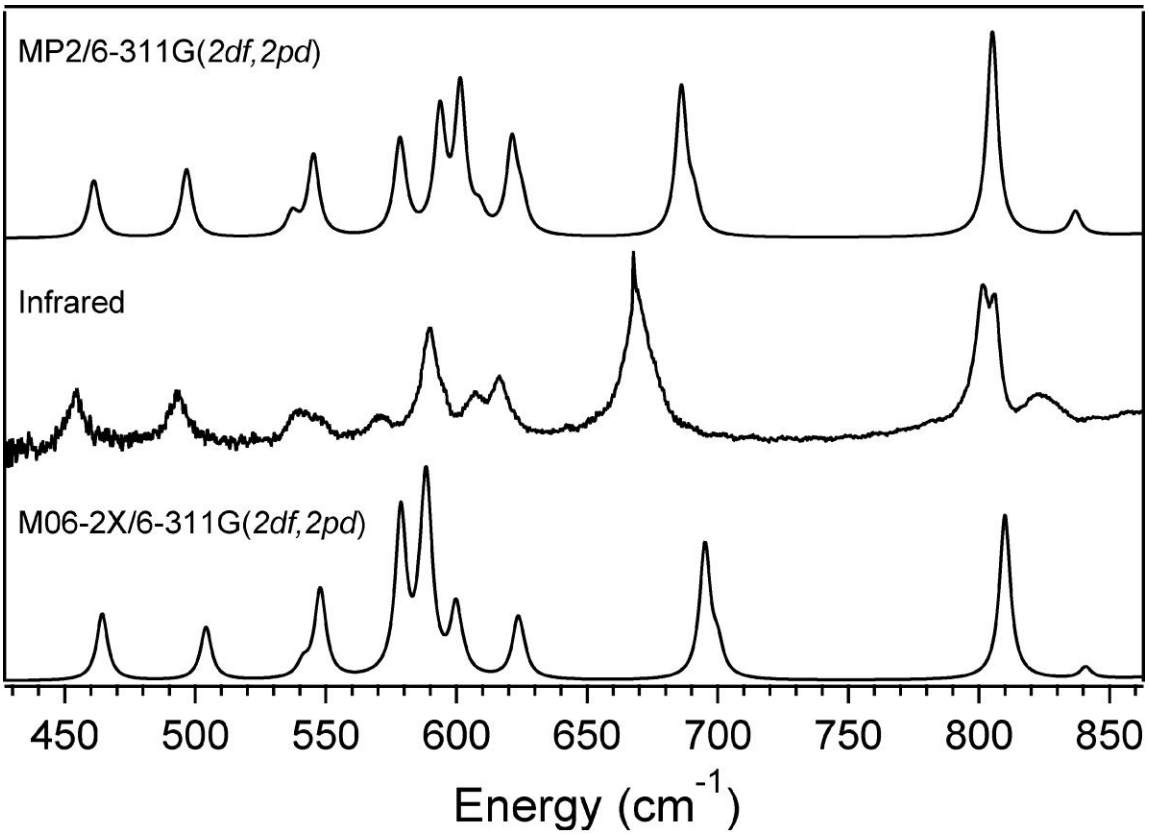

Figure 2.6 Detailed comparison of experimental and theoretical Infrared spectra.

cm^{-1}, slightly below the computed harmonic value of 579 cm^{-1}. Although these results preclude a definitive assignment of the B-N stretching mode, the correlation between the computed spectra and experimentally observed peaks strongly suggest that the vibrational mode dominated by the B-N stretch is one of the four peaks in the range 560-650 cm^{-1}. This observation makes it one of the lowest, if not the lowest, energy vibrations observed to date that can be primarily attributed to B-N stretching.

2.5 Conclusions

Comparison of experimental infrared, Raman, and SERS spectra of methylboronic acid MIDA ester with theoretical predictions suggests that the vibrational mode with the most significant B-N dative bond stretching character in this molecule occurs in the range 560-650 cm^{-1}. In MBA MIDA ester, this mode is very localized and predominantly due to one motion, a surprising result for such a large and constrained molecule. This spectral assignment makes it one of the lowest, if not the lowest, experimentally observed B-N stretching modes. SERS spectra also exhibit an enhanced peak at 1126 cm^{-1}, indicating a possible interaction of the nitrogen atom with the silver surface.

This work was published in the *Journal of Physical Chemistry A*, and it was featured on the cover of the June 23, 2011 issue, shown in Figure 2.7.

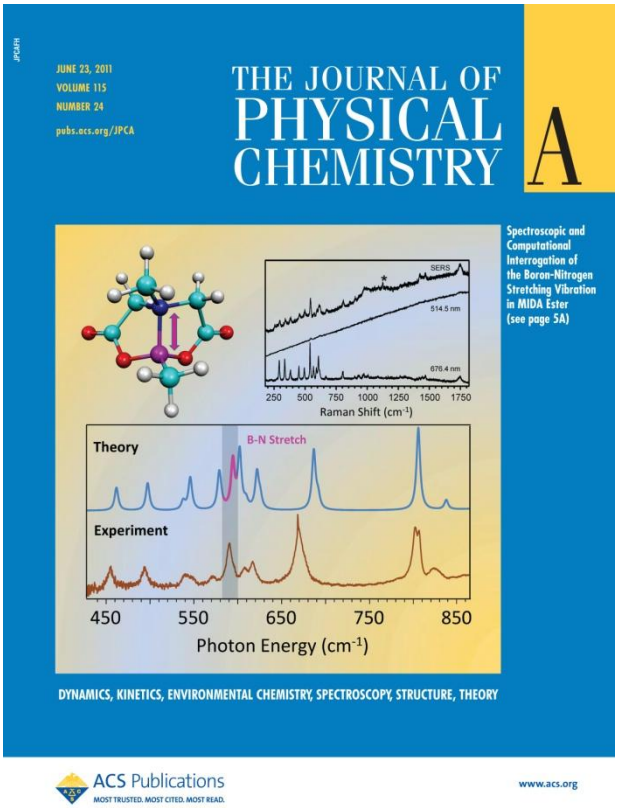

Figure 2.7 Cover of the *Journal of Physical Chemistry A*, June 23, 2011 issue.

2.6 References

(1) Uno, B. E.; Gillis, E. P.; Burke, M. D. *Tetrahedron***2009**, 65, 3130–3138.

(2) Gillis, E. P.; Burke, M. D. *J. Am. Chem. Soc.***2008**, 130, 14084–14085.

(3) Knapp, D. M.; Gillis, E. P.; Burke, M. D. *J. Am. Chem. Soc.***2009**, 131, 6961–6963.

(4) Hughes, E. W. *J. Am. Chem. Soc.***1956**, 78, 502–503.

(5) Rice, B.; Galiano, R. J.; Lehmann, W. J. *J. Phys. Chem.***1957**, 61, 1222–1226.

(6) Taylor, R. C.; Cluff, C. L. *Nature* (London, U. K.) **1958**, 182, 390–391.

(7) Goubeau, J. *Adv. Chem. Ser.* **1964**, 42, 87–94.

(8) Taylor, R. C. *Adv. Chem. Ser.* **1964**, 42, 59–70.

(9) Sawodny, W.; Goubeau, J. *Z. Phys. Chem.* (Muenchen, Ger.) **1965**, 44, 227–241.

(10) Kuznesof, P. M.; Shriver, D. F.; Stafford, F. E. *J. Am. Chem. Soc.* **1968**, 90, 2557–2560.

(11) Moireau,M.C.; Veillard, A. *Theor. Chem. Acta* **1968**, 11, 344–357.

(12) Smith, J.; Seshadri, K. S.; White, D. *J. Mol. Spectrosc.***1973**, 45, 327–337.

(13) Odom, J. D.; Barnes, J. A.; Hudgens, B. A.; Durig, J. R. *J. Phys. Chem.* **1974**, 78, 1503–1509.

(14) Hu, M. G.; Geanangel, R. A. *Inorg. Chem.* **1979**, 18, 3297–301.

(15) Zirz, C.; Ahlrichs, R. *J. Chem. Phys.* **1981**, 75, 4980–4982.

(16) Reuter, D. C.; Thorne, L. R.; Gwinn, W. D. *J. Phys. Chem.* **1982**, 86, 4737–4745.

(17) Binkley, J. S.; Thorne, L. R. *J. Chem. Phys.* **1983**, 79, 2932–2940.

(18) Thorne, L. R.; Suenram, R. D.; Lovas, F. J. *J. Chem. Phys.* **1983**,

78, 167–171.

(19) Marsh, C. M. B.; Hamilton, T. P.; Xie, Y.; Schaefer, I.; Henry, F. *J. Chem. Phys.* **1992**, 96, 5310–5317.

(20) Bauschlicher, J.; Charles, W.; Ricca, A. *Chem. Phys. Lett.* **1995**, 237, 14–19.

(21) Leboeuf, M.; Russo, N.; Salahub, D. R.; Toscano, M. *J. Chem. Phys.* **1995**, 103, 7408–7413.

(22) Richardson, T.; de Gala, S.; Crabtree, R. H.; Siegbahn, P. E. M. *J. Am. Chem. Soc.* **1995**, 117, 12875–12876.

(23) Vijay, A.; Sathyanarayana, D. N. *Chem. Phys.* **1995**, 198, 345–352.

(24) Hu, R.; Chung, T. C. *Carbon* **1996**, 34, 595–600.

(25) Toyota, S.; Futawaka, T.; Asakura, M.; Ikeda, H.; Oki, M. *Organometallics* **1998**, 17, 4155–4163.

(26) Fisher, L. S.; McNeil, K.; Butzen, J.; Holme, T. A. *J. Phys. Chem. B* **2000**, 104, 3744–3751.

(27) Flores-Parra, A.; Contreras, R. *Coord. Chem. Rev.* **2000**, 196, 85–124.

(28) Fisher, L.; Holme, T. J. *Comput. Chem.* **2001**, 22, 913–922.

(29) Merino, G.; Bakhmutov, V. I.; Vela, A. *J. Phys. Chem. A* **2002**, 106, 8491–8494.

(30) Custelcean, R.; Dreger, Z. A. *J. Phys. Chem. B* **2003**, 107, 9231–9235.

(31) Dillen, J.; Verhoeven, P. *J. Phys. Chem. A* **2003**, 107, 2570–2577.

(32) Trudel, S.; Gilson, D. F. R. *Inorg. Chem.* **2003**, 42, 2814–2816.

(33) Allis, D. G.; Kosmowski, M. E.; Hudson, B. S. *J. Am. Chem. Soc.* **2004**, 126, 7756–7757.

(34) Gilbert, T. M. *J. Phys. Chem. A* **2004**, 108, 2550–2554.

(35) Mitrasinovic, P. M. *Chem. Phys. Lett.* **2004**, 392, 419–427.

(36) Mo, Y.; Song, L.; Wu, W.; Zhang, Q. *J. Am. Chem. Soc.* **2004**, 126, 3974–3982.

(37) Morrison Carole, A.; Siddick Muhammad, M. *Angew. Chem., Int. Ed.* **2004**, 43, 4780–4782.

(38) Sinha, P.; Boesch, S. E.; Gu, C.; Wheeler, R. A.; Wilson, A. K. *J. Phys. Chem. A* **2004**, 108, 9213–9217.

(39) LeTourneau, H. A.; Birsch, R. E.; Korbeck, G.; Radkiewicz-Poutsma, J. L. *J. Phys. Chem. A* **2005**, 109, 12014–12019.

(40) Meng, Y.; Zhou, Z.; Duan, C.; Wang, B.; Zhong, Q. *THEOCHEM* **2005**, 713, 135–144.

(41) Zhu, L.; Shabbir, S. H.; Gray, M.; Lynch, V. M.; Sorey, S.; Anslyn, E. V. *J. Am. Chem. Soc.* **2006**, 128, 1222–1232.

(42) Bowden, M. E.; Gainsford, G. J.; Robinson, W. T. *Aust. J. Chem.* **2007**, 60, 149–153.

(43) Li, J.; Kathmann, S. M.; Schenter, G. K.; Gutowski, M. *J. Phys. Chem. C* **2007**, 111, 3294–3299.

(44) Liao, H.-Y. Int. *J. Quantum Chem.* **2007**, 108, 84–89.

(45) Mohri, F.; Granovsky, A. A. Int. *J. Quantum Chem.* **2007**, 108, 544–557.

(46) Nguyen, V. S.; Matus, M. H.; Grant, D. J.; Nguyen, M. T.; Dixon, D. A. *J. Phys. Chem. A* **2007**, 111, 8844–8856.

(47) Plumley, J. A.; Evanseck, J. D. *J. Phys. Chem. A* **2007**, 111, 13472–13483.

(48) Roy, C. D.; Brown, H. C. *J. Organomet. Chem.* **2007**, 692, 784–790.

(49) Hess, N. J.; Bowden, M. E.; Parvanov, V. M.; Mundy, C.; Kathmann, S. M.; Schenter, G. K.; Autrey, T. *J. Chem. Phys.* **2008**, 128, 034508.

(50) Hess, N. J.; Hartman, M. R.; Brown, C. M.; Mamontov, E.; Karkamkar, A.; Heldebrant, D. J.; Daemen, L. L.; Autrey, T. *Chem. Phys. Lett.* **2008**, 459, 85–88.

(51) Larkin, J. D.; Milkevitch, M.; Bhat, K. L.; Markham, G. D.; Brooks, B. R.; Bock, C. W. *J. Phys. Chem. A* **2008**, 112, 125–133.

(52) Goubeau, J.; H., M. *Z. Phys. Chem.* **1958**, 14, 61.

(53) Luther, H.; Mootz, D.; Radwitz, F. *J. Prakt. Chem.* **1958**, 5, 242–259.

(54) Goubeau, J.; Becher, H. *Z. Anorg. Allgem. Chem.* **1952**, 268, 1–12.

(55) Popelier, P. L. A. *J. Phys. Chem. A* **1998**, 102, 1873–1878.

(56) Klooster, W. T.; Koetzle, T. F.; Siegbahn, P. E. M.; Richardson, T. B.; Crabtree, R. H. *J. Am. Chem. Soc.* **1999**, 121, 6337–6343.

(57) Becke, A. *J. Chem. Phys.* **1993**, 98, 5648–5652.

(58) Lee, C.; Yang, W.; Parr, R. G. *Phys. Rev. B* **1988**, 37, 785–789.

(59) Zhao, Y.; Truhlar, D. G. *Theor. Chem. Acc.* **2008**, 120, 215–241.

(60) Plumley, J. A.; Evanseck, J. D. *J. Chem. Theory Comput.* **2008**, 4, 1249–1253.

(61) Janesko, B. G. *J. Chem. Theory Comput.* **2010**, 6, 1825–1833.

(62) Moller, C.; Plesset, M. S. *Phys. Rev.* **1934**, 46, 618–622.

(63) Frisch, M. J. Gaussian 09, Revision A.2; Gaussian Inc.: Wallingford, CT, **2009**.

(64) INTDER2005 is a general program developed by Wesley D. Allen and co-workers that performs various vibrational analyses and higher-order nonlinear transformations among force field representations.

(65) Zhao, J.; Lui, H.; McLean, D. I.; Zeng, H. *Appl. Spectrosc.* **2007**, 61, 1225–1232.

(66) Ruperez, A.; Laserna, J. J. *Appl. Spectrosc.* **1994**, 48, 219–223.

(67) Maruyama, Y.; Futamata, M. *Chem. Phys. Lett.* **2005**, 412, 65–70.

(68) Mahajan, S.; Cole, R. M.; Speed, J. D.; Pelfrey, S. H.; Russell, A. E.; Bartlett, P. N.; Barnett, S. M.; Baumberg, J. J. *J. Phys. Chem. C* **2010**,

114, 7242–7250.

(69) Shegai, T. O.; Haran, G. *J. Phys. Chem. B* **2006**, 110, 2459–2461.

(70) Podstawka, E.; Olszewski, T. K.; Boduszek, B.; Proniewicz, L. M. *J. Phys. Chem. B* **2009**, 113, 12013–12018.

(71) Pagliai, M.; Muniz-Miranda, M.; Cardini, G.; Schettino, V. *J. Phys. Chem. A* **2009**, 113, 15198–15205.

3 Elucidation of the B-P Dative Bond Stretching Frequency

3.1 Introduction

To further the study of dative bond stretching frequencies, boron-phosphorus dative bonds are studied. There has already been an extensive experimental study of boron-phosphorus dative bond containing molecules using a variety of methods.[1-34] However, understanding the properties of the boron-phosphorus dative bond stretching frequency has been a challenge to chemists for many years because of the inconclusive results obtained in the studies. The NMR, microwave, infrared, and Raman spectra of many B-P containing molecules in the solid, liquid, and gas phases have been studied in a series by Odom and Durig[1-22, 24-26, 28]. In these studies, data regarding barriers to internal rotation, dipole moments, conformational stability, and normal coordinate analyses were obtained in an attempt to describe each structure. Before the series studied by Odom and Durig, Rudolph studied the structure of phosphine borane (H_3PBH_3), determining that the B-P coupling constant was a good qualitative measure of dative bond strength.[23] In 1973, Durig and Odom begin their series of studies of B-P dative bonded molecules.[24] In studying the vibrational spectra of trimethylphosphine borane ($(H_3C)_3PBH_3$), the B-P mode was observed as a doublet, and it was suggested that the mode is strongly mixed with C-P symmetric stretching motions from the author's potential energy distribution calculations. In 1974, dimethylphosphine borane was studied.[25] Durig and coworkers concluded that B-P and B-N stretching frequencies behave differently upon methyl

substitution of the Group V element. The B-N stretching frequency decreases linearly with methyl substitution from ammonia borane to trimethylamine borane while the B-P stretching frequency is unaffected by methyl substitution from methylphosphine borane to trimethylphosphine borane. In 1987, Odom et al. continued the studies with methyldifluorophosphine borane, saying that the increased methyl substitution of the phosphorus atom in B-P molecules leads to greater thermal stability.[26] Also, the authors noted that "despite the large amounts of structural and physical data, attempts to correlate structures and stability of phosphorus-boron adducts have not been very successful," and that B-P bonds do not appear to follow a trend like B-N bonds.

In 1993, Van der Veken continued the series of studies on phosphorus-boron compounds by adding ab initio calculations to the analysis of spectra of (chloromethyl)difluorophosphine borane.[27] HF/3-21G* and HF/6-31G* computations were used to analyze the B-P bond in this molecule. He observed that both basis sets predict that the B-P stretch is a relatively pure mode. He also found ab inito calculations to be an "invaluable tool" in deciphering the spectra below 1000 cm^{-1} where the potential energy distributions show coupling among the vibrational modes. Even though 3-21G* is a small basis set, the frequencies for the fundamentals were predicted reasonably well with 2 scaling factors (0.9 for stretching coordinates and 0.8 for bending). Pointing out that there is very limited data available on the structure of B-P molecules in the gas phase, he suggested that it would be useful to determine the outlying values needed for 6-31G* to predict the experimental values from the ab initio values. He also said that it would be of interest to carry out ab initio calculations that include electron correlation to see what parameters would change.

In 1996, Durig conducted his own ab intio study of phosphine boranes.[28] He stated that there was not a clear relationship between chemical stabilities and bond lengths of the complexes he studied, BH_3PH_3, BH_3PHF_2, and BH_3PF_3. Difluorophosphine borane exhibits an unusual stability towards dissociation compared to trifluorophosphine borane even though they have almost identical B-P bond distances, 1.832 Å and 1.836 Å, respectively. He also stated that even though theoretical studies have been performed, the calculations therein suffered from either relatively small basis sets or not taking into account electron correlation. Anane in 1998 carried out an ab initio molecular orbital study of the substituent effect on a variety of phosphine borane complexes employing MP2/6-311G(d,p).[29] They found that bond length decreases with increasing methyl substitution on the phosphorus atom and increases with increasing substitution on the boron atom.

Robb studied the conformational stability of ethyldifluorophosphine borane from temperature-dependent FT-IR spectra of xenon solutions and compared them to MP2/6-31G* calculations.[30] He observed that the methyl barrier to internal rotation is in "excellent" agreement with the experimental one, but the predicted value of the BH_3 barrier is underestimated. He said that part of the difference may be due to the fact that the structural parameters of the borane moiety are not as well predicted as those of the methyl group because of its dative bond nature. He encountered errors in predicting fundamental frequencies on the average of 23 cm^{-1}, employing a single scale factor of 0.9 with MP2/6-31G*.

In 2004, Jensen analyzed the vibrational frequencies and structure of trifluorophosphine borane employing HF, B3LYP, and MP2 methods with the 6-311G**

basis set and comparing those results to already available experimental results.[31] Based on their comparison of results, they developed correction factors for HF, B3LYP, and MP2 of 1.0359, 1.0539, and 0.9902, respectively. In 2006, Bessac et al. studied the chemical bonding in phosphane and amine complexes of main group elements and transition metals.[32] He stated that the bond dissociation energy is not a good measurement of the intrinsic strength of Lewis acidity and basicity of the complex. He also found that the theoretical bond dissociation energies of B-P complexes are smaller than B-N complexes. For instance, BH_3PMe_3 has the largest bond dissociation energy of the complexes he studied, but it does not have the shortest B-P bond length.

Nemeth in 2008 performed a quantum chemical study of phosphine borane complexes by selectively trapping them vacuum. A kinetic stability lower than that of their respective free systems was observed. He found that the complexation energies differ with different methods.[33] Employing B3LYP and MP2, he found that MP2 gave around 10 kJ/mol higher in energy. In 2010, Janesko performed a study in modeling dative bonding in substituted boranes.[34] In reviewing the history of the study, it was stated that B3LYP cannot reproduce accurate B-N bond lengths and bond dissociation energies for several species. Phillips and Cramer found that hybrid DFT functional were required to reliably model the dative bond. Plumley and Evanseck found B3LYP to completely fail at predicting B-N dative bond properties such as bond length and stretching frequency.[35] Of the functionals tested by the authors, only the highly parameterized Minnesota functionals predict the experimental trends well. From this, it is recommended to use the M06-2X method. Global hybrid density functionals like MPW1K and M06-2X have a relatively large computational cost due, consisting of exact

HF type exchange. Janesko employed PBEsol GGA with either aug-cc-pVTZ or 6-311++G(3df,2p) to try and reproduce the accuracy of MPW1K and M06-2X with a lesser computational cost.[34] PBEsol GGA gives fairly accurate energies and "reasonable, though overbound" geometries for a range of dative bonds.

In this study, we present experimental Raman spectra of B-P containing molecules that have large functional groups. These include diphenylphosphine borane, triphenylphosphine borane, and di(*tert*-butyl)phosphine borane. The structures of the three B-P containing molecules are presented in Figure 3.1. The Raman spectra of these molecules have not been previously published in the literature. We compare our experimental spectra with results of ab initio calculations using the M06-2X method and different sized basis sets to fully describe the nature of the boron-phosphorus dative bond by examining the B-P stretching frequency in each case. We also theoretically compare sixteen additional previously studied B-P containing molecules.

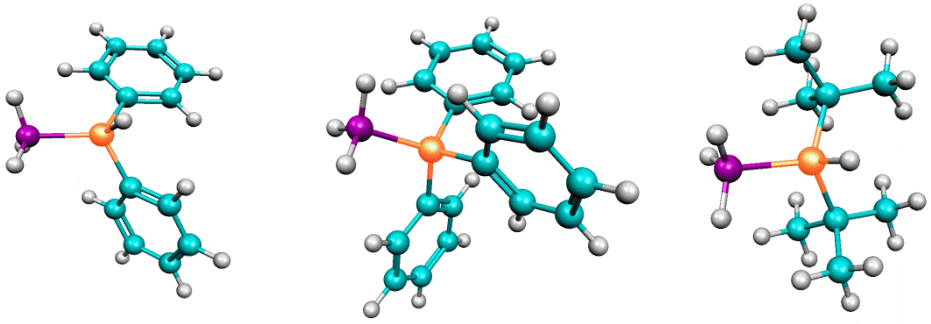

Figure 3.1 Molecules that contain a B-P dative bond: diphenylphosphine borane (left), triphenylphosphine borane (middle), and di(*tert*-butyl)phosphine borane (right).

3.2 Spectroscopic Methods

Diphenylphosphine borane, triphenylphosphine borane, and di(tert-butyl)phosphine borane were obtained from Sigma-Aldrich and were used for the Raman experiment presented here without any further purification. Raman spectra of these three molecules

were obtained using the 514.5 nm laser line from argon or krypton ion lasers. A Ramanor HG2-S Raman scanning spectrometer was employed to acquire Raman spectra using the 514.5 nm line from an Ar ion laser. A Nachet NS 400 micro-Raman setup was used to analyze the sample with an incident laser power of 300 mW at the sample, and a 0.5 cm^{-1}/s scan speed was employed over the range 0-3500 cm^{-1}. Spectra were acquired and interpreted using a custom computer program written using National Instruments LabView.

3.3 Theoretical Methods

The Gaussian 09 software package was employed to optimize the structure and to calculate the unscaled harmonic vibrational frequencies as well as the corresponding Raman intensities of diphenylphosphine borane and di(*tert*-butyl)phosphine borane. The M06-2X global hybrid density functional[36] was used in conjunction with the split-valence basis sets 6-31G, 6-31G(d,p), 6-311G(*2df,2pd*), aug-cc-pVDZ, and aug-cc-pVTZ. Harmonic vibrational frequencies computed at the same level of theory confirmed that each optimized geometry corresponds to a minimum on the potential energy surface. Default convergence criteria were employed in each calculation. Simulated spectra were created by combining Lorentzians for each normal mode using a custom program developed with National Instruments LabView. The INTDER2005 program[37] was employed to determine the total energy distributions (TEDs) characterizing the normal modes. The B-P stretch is defined as the simple internal coordinate S_1 = r(B-P).

3.4 Results and Discussion

Experimental Raman spectra of di(*tert*-butyl)phosphine borane, diphenylphosphine borane, and triphenylphosphine borane are presented in Figure 3.2 A comparison of the experimental and theoretical results obtained for di(*tert*-butyl)phosphine borane, diphenylphosphine borane, and triphenylphosphine borane is presented in Figures 3.3 - 3.6 When the theoretical results are compared to the experimental results, there is good agreement between all modes, including in the B-P stretching region. The triple zeta basis set yielded similar results as the quadruple zeta basis set, at a fraction of the computational cost. It was also determined that diffuse functions are not required to accurately describe the experimental spectra, also reducing computational cost.

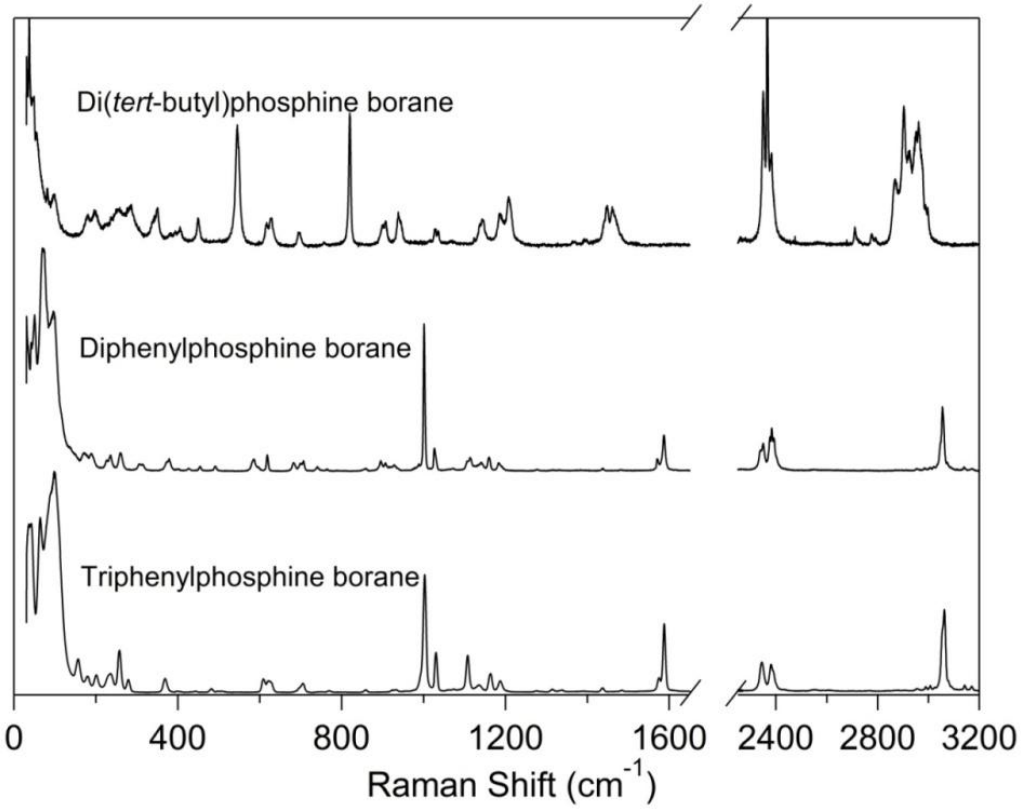

Figure 3.2 Comparison of the experimental Raman spectra of diphenylphosphine borane, triphenylphosphine borane, and di(*tert*-butyl)phosphine borane.

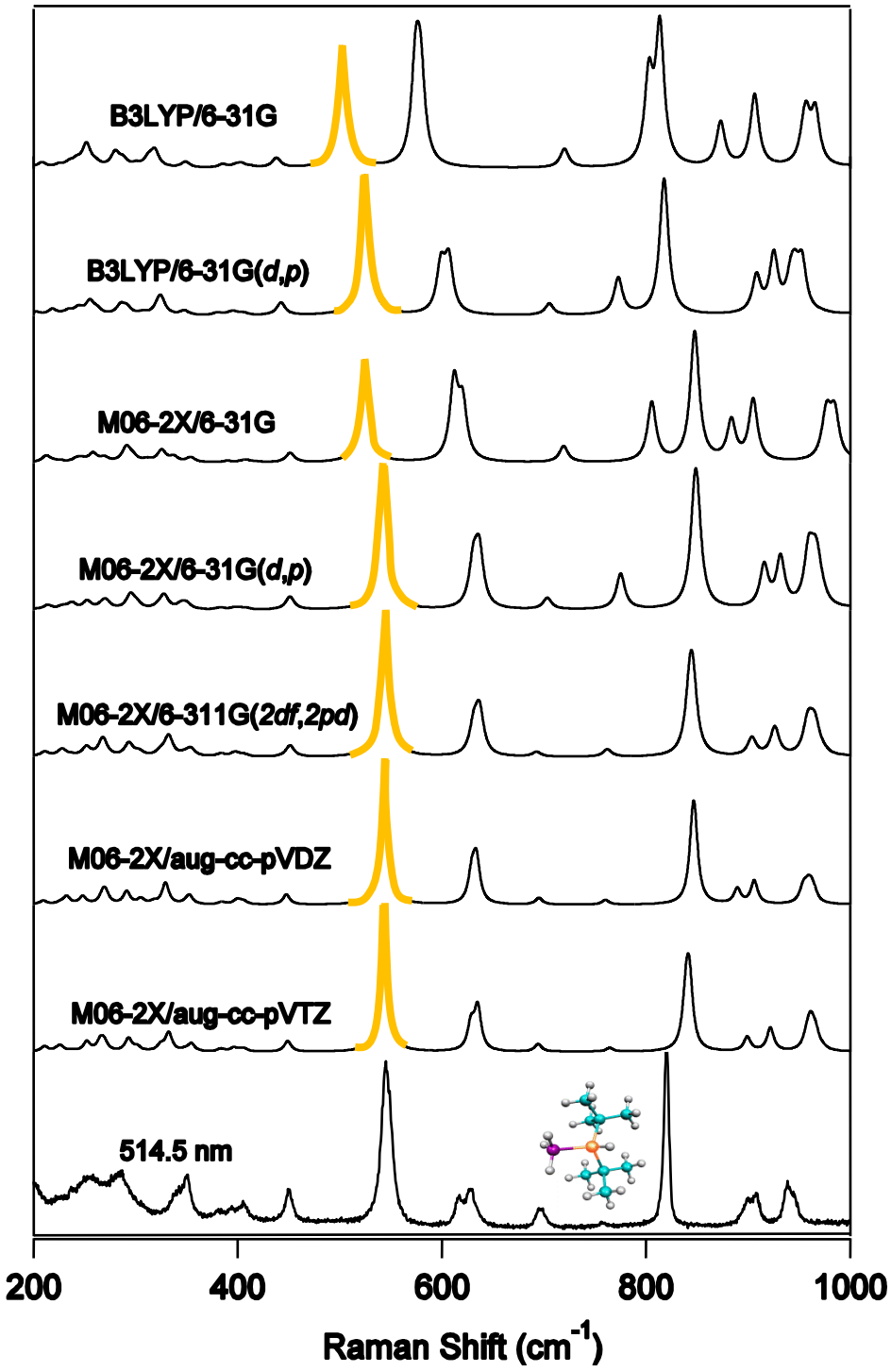

Figure 3.3 Comparison of experimental Raman spectra of di(*tert*-butyl)phosphine borane to various levels of theory. The B-P stretch is highlighted in orange.

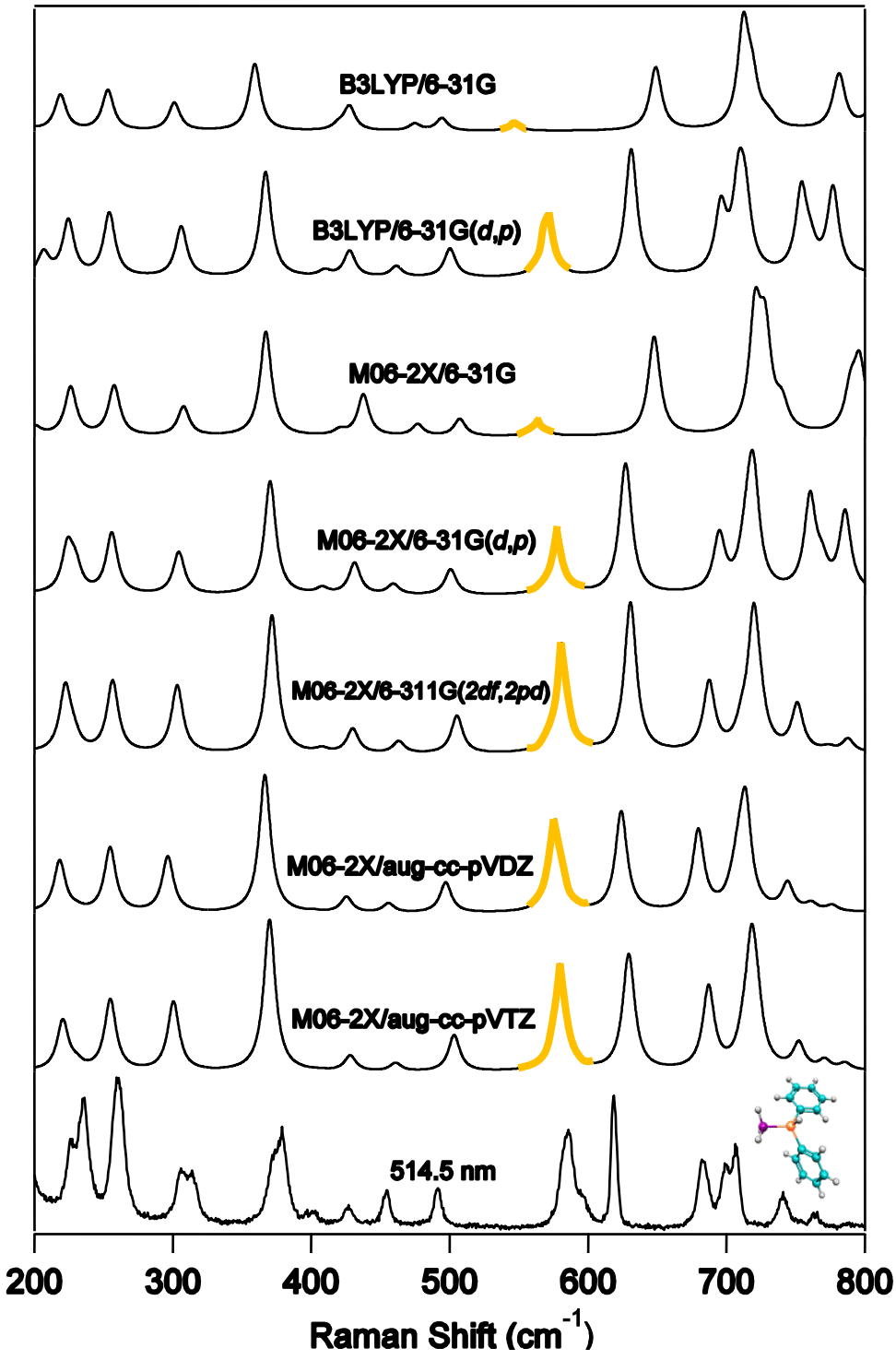

Figure 3.4 Comparison of experimental Raman spectra of diphenylphosphine borane to various levels of theory. The B-P stretch is highlighted in orange.

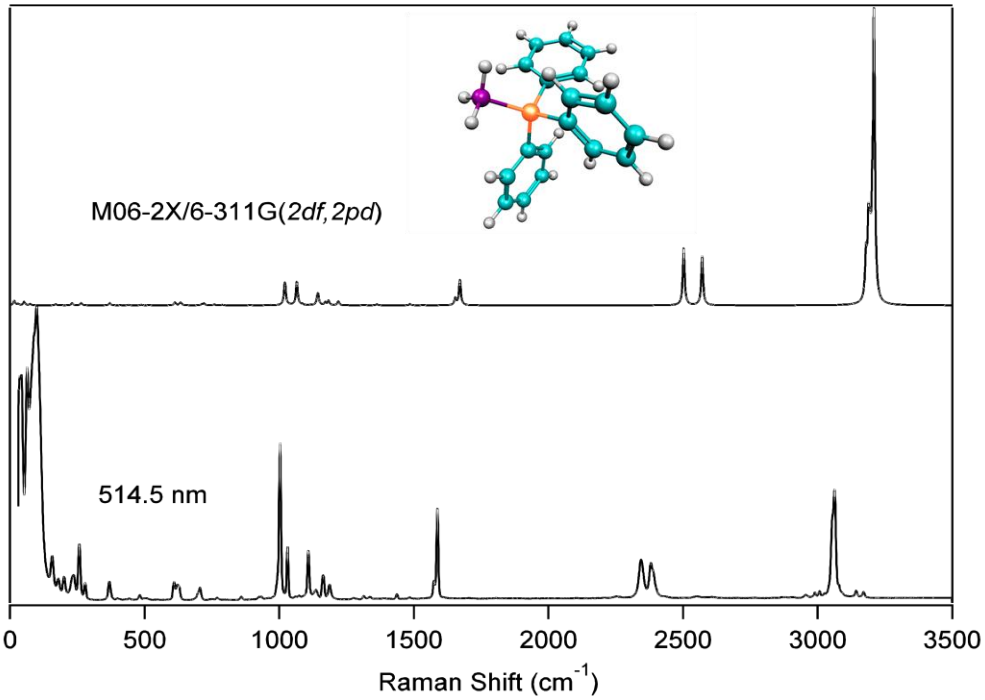

Figure 3.5 Comparison of experimental Raman spectra of triphenylphosphine borane to a simulated spectrum at the M06-2X/6-311G(*2df,2pd*) level of theory.

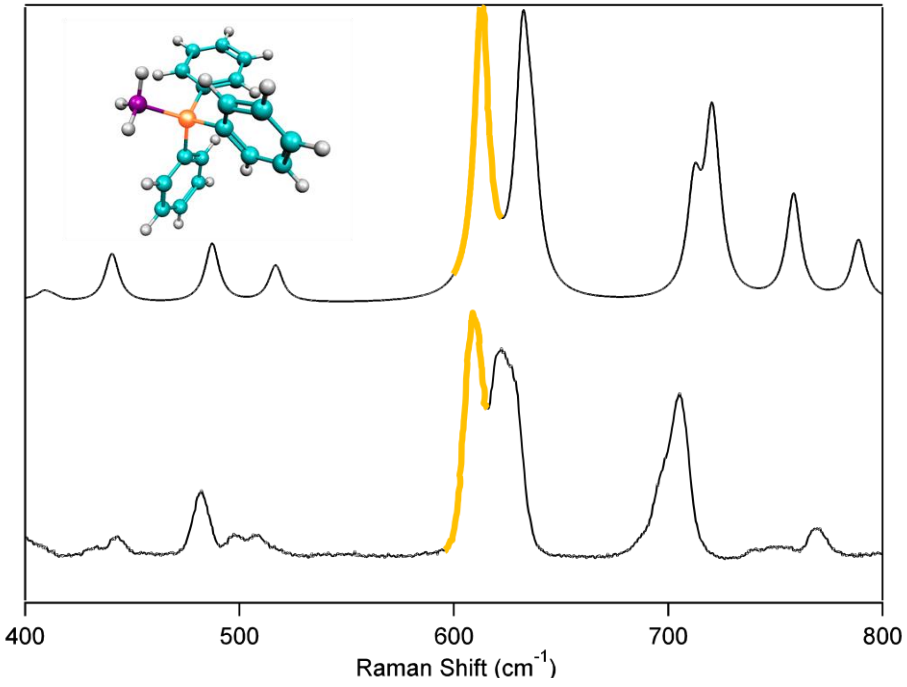

Figure 3.6 Comparison of experimental Raman spectra of triphenylphosphine borane to simulated spectrum at the M06-2X/6-311G(*2df,2pd*) level of theory. The B-P stretch is highlighted in orange.

In an effort to better understand structural influences on B-P stretching frequencies, the M06-2X method with the 6-311G(*2df,2pd*) basis set was employed to optimize the geometries and calculate the Raman frequencies and intensities for 16 previously experimentally studied molecules.

Molecule	r(B-P) (Å) Calculated*	r(B-P) (Å) Previous Assignments**	ν(B-P) (cm^{-1}) Calculated*	ν(B-P) (cm^{-1}) Previous Assignments**
H_3P-BH_3	1.935	1.937[9]	522	562 (s)[9]
$CH_3CH_2PH_2$-BH_3	1.924	1.914[14]	537	556 (l); 558 (s)[14]
CH_3PH_2-BH_3	1.922	1.929[8]	538	560 (l); 572 (s)[8]
$(CH_3CH_2CH_2CH_2)_2PH$ –BH_3	1.936	-	545	545 (s)†
$(CH_3)_2PH$-BH_3	1.914	1.919[4]	548	571 (l)[4]
$(CH_3)_3P$-BH_3	1.909	1.913[2]	553	583 (s)[2]
$(CH_3CH_2)(CH_3)_2P$-BH_3	1.912	-	561	567 (l); 565 (s)[16]
$(Ph)_2PH$-BH_3	1.924	-	581	581 (s)†
$(CH_3)_2ClP$-BH_3	1.896	-	582	-
CH_3F_2P-BH_3	1.855	1.841[17]	584	588 (g); 592 (l); 594 (s)[17]
CH_2ClF_2P-BH_3	1.854	1.817 [trans]; 1.821 [gauche][27]	610	570 (g); 572 (l) [trans] 624 (g); 623 (l) [gauche][27]
$(Ph)_3P$-BH_3	1.928	-	613	613 (s)†
F_3P-BH_3	1.846	1.836[31]	624	585 [HF], 575 [B3LYP], 612 [MP2] / 6-311G** [31]
H_3P-BCl_3	1.996	1.940[1]	626	699 (s)[1]
$CH_3CH_2F_2P$-BH_3	1.856	1.861 [trans][15]	627	617 (g); 616 (l); 615 (s); 632 [trans] MP2/6-31G* [15]
$CH_3CH_2Cl_2P$-BH_3	1.895	-	636	537 (l); 534 (s)[18]
H_3P-$B(CH_3)_3$	2.047	2.019[29]	679	-
$(CH_3)_3P$-$B(CH_3)_3$	1.979	-	694	-
$(CH_3)_3P$-BCl_3	1.959	1.957[11]	767	755 (s)[11]

Table 3.1 Boron-phosphorus stretching frequencies and bond lengths for various B-P containing molecules previously studied in the literature. *Calculated in this study with M06-2X/6-311G(*2df,2pd*); **Literature sources cited in table; †Assigned in this study.

The systematic substitution of functional groups on the phosphorus atom has the effect of increasing the B-P stretching frequency with increasing total mass of the substituents. In fact, there is a linear trend within different classes of substituents. This trend is predicted from Equation 1.6 for normal modes with the same force constant but different reduced masses. Figure 3.7 compares the B-P stretching frequency as a function of the square root of reduced mass for methyl-substituted phosphine boranes (left) and for the three molecules with large substituents studied here (right). Although in each case there is a remarkable linear trend, the slope (and thus the force constant) differs between the two different molecular classes. This effect is closely connected to the degree of mixing between the B-P stretch and other normal modes localized on the substituents.

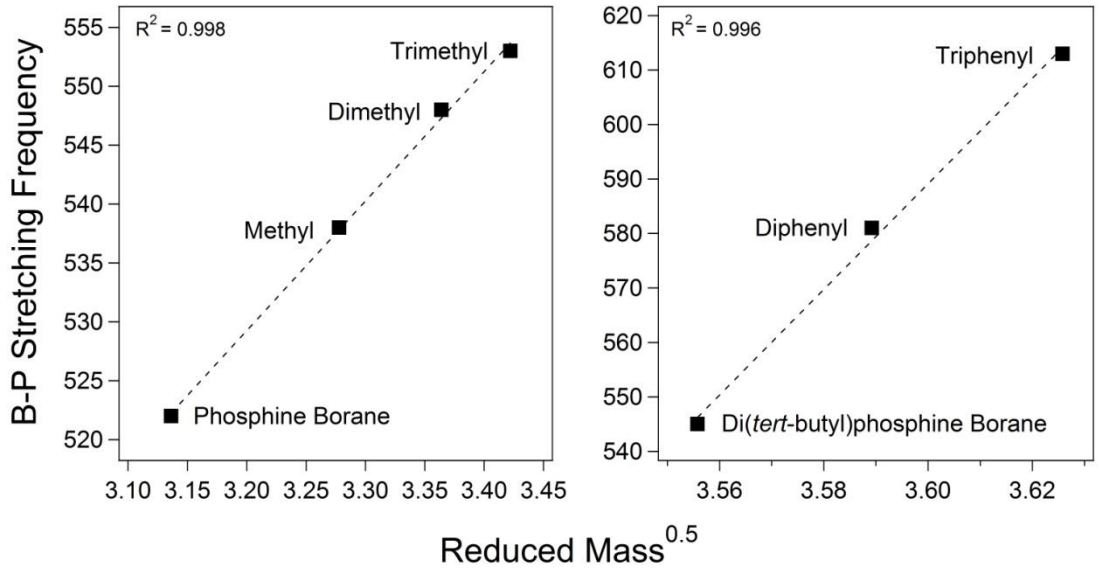

Figure 3.7 Linear trends of theoretical B-P stretching frequencies as a function of the square root of the reduced masses for methyl substituted phosphine boranes (left) and di(-*tert*-butyl)phosphine borane, diphenylphosphine borane, and triphenylphosphine borane (right).

To quantify this substitution effect, total energy distributions for each molecule considered here will be calculated and the degree of mixing within different molecular

classes will be determined. The INTDER2005 program will be employed to perform the TEDs for each of the molecules. These studies will help elucidate where and what percentage of the B-P stretching frequency is in each different molecule, and based on how the molecule is substituted, a predictive trend of the B-P dative bond's physical properties can be developed. Preliminary results show that molecules with substitution on the phosphorus atom have a much lower B-P stretching frequency than structures with substitution on the boron atom. The substituent itself and the symmetry of the substitution also have significant effects on the location of the B-P stretch.

3.5 Conclusions

The experimental results for di(*tert*-butyl)phosphine borane, diphenylphosphine borane, and triphenylphosphine borane match closely with theoretical results employing the M06-2X method with a triple zeta basis set. This good agreement allow for the assignments of the B-P stretching frequency in each case and a comparison to previous results from the literature. Preliminary TED results show that the B-P stretch is fairly localized. In the systematic study of B-P containing molecules, molecules with substitution on the phosphorus atom have a much lower B-P stretching frequency than structures with substitution on the boron atom. The substituent itself and the symmetry of the substitution also have significant effects on the frequency of the B-P stretch. This work is currently being written as a series of two manuscripts, with one to be submitted to the journal *Inorganic Chemistry* in the near future.

3.6 References

(1) Odom, J. D., Riethmiller, S., Witt, J. D., Durig, J. R., *Inorg. Chem.*, **1973**.

(2) Odom, J. D., Hudgens, B. A., Durig, J. D., *J. Phys. Chem.*, **1973**.

(3) Black, D. L., Taylor, R.C., *Acta Cryst.*, **1974**.

(4) Durig, J. R., Hudgens, B. A., Li, Y. S., Odom, J. D., *J. Chem. Phys.*, **1974**.

(5) Durig, J. R., Riethmiller, S., Kalasinsky, V. F., Odom, J. D., *Inorg. Chem.*, **1974**.

(6) Odom, J. D., Hudgens, B. A., Durig, J. R., *J. Phys. Chem.*, **1974**.

(7) Odom, J. D., Kalasinsky, V. F., Durig, J. R., *Inorg. Chem.*, **1974**.

(8) Durig, J. R., Kalasinsky, V. F., Li, Y. S., Odom, J. D., *J. Phys. Chem.*, **1975**.

(9) Odom, J. D., Kalasinsky, V. F., Durig, J. R., *J. Mol. Struc.*, **1975**.

(10) Odom, J. D., Kalasinsky, V. F., Durig, J. R., *Inorg. Chem.*, **1975**.

(11) Drake, J. E., Hencher, J. L., Rapp, B., *Inorg. Chem.*, **1976**.

(12) Durig, J. R., Brletic, P. A., Li, Y. S., Johnston, S. A., Odom, J. D., *J. Chem. Phys.*, **1981**.

(13) Taylor, R. C., Dunning, V. D., *J. Mol. Struc.*, **1982**.

(14) Odom, J. D., Brletic, P. A., Johnston, S. A., Durig, J. R., *J. Mol. Struc.*, **1983**.

(15) Durig, J. R., Rizzolo, J. J., Sullivan, J. F., Cheng, M. S., Hizer, T. J., Odom, J. D., *J. Mol. Struc.*, **1987**.

(16) Durig, J. R., Hizer, T. J., Odom, J. D., *J. Mol. Struc.*, **1987**.

(17) Odom, J. D., Stanley, A. E., Cheng, M. S., Durig, J. R., *J. Raman Spec.*, **1987**.

(18) Odom, J. D., Hizer, T. J., Stanley, A. E., Tonker, T. L, Durig, J. R., *Spec. Acta.*, **1987**.

(19) Iijima, K., Hakamata, Y., Nishikawa, T., Shibata, S., *Chem. Soc. Japan*, **1988**.

(20) Pestana, D. C., Power, P. P., *J. Am. Chem. Soc.*, **1991**.

(21) Allen, T. L, Fink, W. H., *Inorg. Chem.*, **1993**.

(22) Durig, J. R., Shen, Z., *Theochem*, **1997**.

(23) Bryan, P.S., Kuckowski, R. L, *Inorg. Chem.*, **1972**.

(24) Durig, J. R., Li, Y. S., Carreria, L. A., Odom, J. D., *J. Am. Chem. Soc.*, **1973**.

(25) Durig, J. R., Hudgens, B. A., Li, Y. S., Odom, J. D., *J. Chem. Phys.*, **1974**.

(26) Odom, J. D., Stanley, A. E., Cheng, M. S., Durig, J. R., *J. Raman Spec.*, **1987**.

(27) Van der Veken, B. J., Sanders, R. S., Harlan, R. J., Durig, J. R., *Spectro. Acta*, **1993**.

(28) Durig, J. R., Shen, Z.,*Theochem*, **1996**.

(29) Anane, H., Jarid, A., Boutalib, A., Nebot-Gil, I., Tomas, F., *Chem. Phys. Letters*, **1998**.

(30) Robb II, J. B., Xiao, J., Durig, J. R., *J. Mol. Struc.*, **1998**.

(31) Jensen, J. O, *Theochem*, **2004**.

(32) Bessac, F., Frenking, G., *Inorg. Chem.*, **2006**.

(33) Nemeth, B., Khater, B., Veszpremi, T., Guillemin, J., *Royal Soc. Chem.*, **2008**.

(34) Janesko, B., *J. Chem. Theor. Comp.*, **2010**.

(35) Plumley, J. A., Evanseck, J. D., *J. Chem. Theor. Comp.*, **2008**.

(36) Zhao, Y.; Truhlar, D. G. *Theor. Chem. Acc.***2008**.

(37) INTDER2005 is a general program developed by Wesley D. Allen and co-workers that performs various vibrational analyses and higher-order nonlinear transformations among force field representations.

Curriculum Vitae

Experience

Undergraduate Research Associate
(2009 - present) University of Mississippi, University, MS

NASA Academy Research Associate
(2010) NASA/Marshall Space Flight Center, Huntsville, AL

Education

University of Mississippi, University, MS
2008 – 2013 (anticipated)
B.S. Chemical Engineering (Honors)
B.S. Chemistry (Honors)

Honors and Awards

Alpha Lambda Delta Honor Society
Barry M. Goldwater Scholarship 2012
Barry M. Goldwater Scholarship Honorable Mention 2011
Mortar Board Senior Honor Society
National Society of Collegiate Scholars
Omicron Delta Kappa Leadership Honor Society
Oral Presentation Award, 3rd place, 2011 AIChE Southeastern Regional Meeting
Phi Kappa Phi Honor Society
Poster Presentation Award, 1st place, 2012 Mississippi State EPSCoR Meeting
Tau Beta Pi Engineering Honor Society
University of Mississippi Outstanding Freshman in Chemical Engineering 2009
University of Mississippi Outstanding Junior in Chemical Engineering 2011
University of Mississippi Outstanding Physical Chemistry Student 2011
University of Mississippi Outstanding ACS Undergraduate Researcher 2011
University of Mississippi Outstanding Senior in Chemical Engineering 2012
University of Mississippi Sally McDonnell Barksdale Honors College
University of Mississippi Chancellor's Honor Roll
University of Mississippi Dean's Honor Roll
Who's Who Among Students in American Colleges and Universities 2011 - 2012

Publications

D. N. Reinemann, A. Wright, J. Wolfe, G. Tschumper, N. Hammer, "Vibrational Spectroscopy of *N*-Methyliminodiacetic acid (MIDA)-Protected Boronate Esters: Examination of the B-N Dative Bond." *Journal of Physical Chemistry A*, 115, 6426-6431 (2011).

Professional Presentations

D. N. Reinemann, A. Wright, G. Tschumper, N. Hammer, "Examination of B-N and B-P Dative Bonds." 2012 Mississippi State EPSCoR Meeting, University, MS April 2012. (1st place undergraduate poster presentation award)

D. N. Reinemann, A. Wright, G. Tschumper, N. Hammer, "Elucidation of the B-N and B-P stretching vibrations in organic molecules," Poster, 242nd National Meeting of the American Chemical Society, Denver, CO, August 2011.

D. N. Reinemann, A. Wright, J. Wolfe, G. Tschumper, N. Hammer, "Vibrational Spectroscopy of *N*-Methyliminodiacetic acid (MIDA)-Protected Boronate Esters: Examination of the B-N Dative Bond." 2012 American Institute of Chemical Engineers (AIChE) Southeastern Regional Meeting, Atlanta, GA April 2011.

J. L. Perry, K. R. Frederick, J. P. Scott, **D. N. Reinemann**, "A Comparison of Photocatalytic Oxidation Reactor Performance for Spacecraft Cabin Trace Contaminant Control Applications." 41st International Conference on Environmental Systems of the American Institute of Aeronautics and Astronautics, Portland, OR, July 2011.

D. N. Reinemann, A. Wright, J. Wolfe, G. Tschumper, N. Hammer, "Vibrational Spectroscopy of *N*-Methyliminodiacetic acid (MIDA)-Protected Boronate Esters: Examination of the B-N Dative Bond." 2011 Mississippi State EPSCoR Meeting, Starkville, MS April 2011.

D. N. Reinemann, A. Wright, J. Wolfe, G. Tschumper, N. Hammer, "Elucidation of the B-N Stretching Vibration in *N*-Methyliminodiacetic acid (MIDA) Boronates." Southeastern Regional Meeting of the American Chemical Society (SERMACS), New Orleans, LA, December 4, 2010.

D. N. Reinemann, A. Wright, J. Wolfe, G. Tschumper, N. Hammer, "Raman and SERS Spectroscopy of *N*-Methyliminodiacetic acid (MIDA)-Protected Boronate Esters." International Conference on Raman Spectroscopy (ICORS), Boston, MA, August 12, 2010.

D. N. Reinemann, J. Perry, "Air Revitalization Using Adsorbent Media for Space Exploration Life Support," 2010 NASA/Marshall Space Flight Center Summer Intern poster session, Huntsville, AL, July 29, 2010.

J. Wolfe, A. Wright, **D. N. Reinemann**, N. Hammer, "Surface Enhanced Raman Scattering (SERS) Spectroscopy of Molecules Containing B–N Dative Bonds," 2010 Mississippi State EPSCoR Meeting, Jackson, MS, April 2010.

D. N. Reinemann, A. Wright, G. Tschumper, N. Hammer, "Computational and Raman Spectroscopic Studies of *N*-Methyliminodiacetic Acid (MIDA)-Protected Boronate Esters." 2010 Mississippi State EPSCoR Meeting, Jackson, MS April 2010.

D. N. Reinemann, A. Wright, A. Howard, G. Tschumper, N. Hammer, "Vibrational Spectroscopy of *N*-Methyliminodiacetic Acid (MIDA)-Protected Boronate Esters: Assignment of the B-N Dative Bond Stretching Frequency." 61st Annual Southeastern Regional Conference of the American Chemical Society (SERMACS), San Juan, Puerto Rico, October 2009.